frontiers | Frontiers in Marine Science

TYPE Original Research
PUBLISHED 27 January 2025
DOI 10.3389/fmars.2025.1505586

OPEN ACCESS

EDITED BY
Sebastian Christoph Alexander Ferse,
IPB University, Indonesia

REVIEWED BY
Yuyuan Xie,
University of South Florida, United States
Peng Zhao,
Hainan University, China

*CORRESPONDENCE
Jing Xia
xiajingsherry@sjtu.edu.cn
Jinlin Liu
jlliu@tongji.edu.cn

RECEIVED 03 October 2024
ACCEPTED 09 January 2025
PUBLISHED 27 January 2025

CITATION
Liu J, Xia Z, Zeng Y, Xia J and He P (2025) Exploration and implication of green macroalgal proliferation in the Nanhui-east-tidal-flat: an investigation of post-reclamation mudflat wetlands.
Front. Mar. Sci. 12:1505586.
doi: 10.3389/fmars.2025.1505586

Exploration and implication of green macroalgal proliferation in the Nanhui-east-tidal-flat: an investigation of post-reclamation mudflat wetlands

Jinlin Liu [1]*, Zhangyi Xia [2], Yinqing Zeng [3], Jing Xia [4,3]* and Peimin He [3]

[1]State Key Laboratory of Marine Geology, Tongji University, Shanghai, China, [2]College of Ocean and Earth Science, Xiamen University, Xiamen, China, [3]College of Oceanography and Ecological Science, Shanghai Ocean University, Shanghai, China, [4]School of Oceanography, Shanghai Jiao Tong University, Shanghai, China

The Nanhui-east-tidal-flat (NETF), the largest marginal shoal in the Yangtze River of China, is significantly impacted by human activities. Prior research has not detected the presence of green macroalgae in the NETF, nor has it explored the effects of reclamation on the distribution of macroalgae. However, in 2021, a small-scale aggregated attached algal mats emerged in the NETF, potentially signaling the onset of a green tide and necessitating vigilant monitoring. Morphological and molecular biological identification analysis revealed that all collected green macroalgae were attributed to a single dominant species, *Ulva prolifera*, characterized by broad blades and prominent air bladders, colonizing various substrates. The attached *U. prolifera* exhibited continuous growth from March to May 2021, peaking at a wet weight of 373.6229 g/m^2 and a dry weight of 72.7904 g/m^2 on May 1, 2021, within the accessible sampling period. The rapid proliferation of the "opportunistic" *Ulva* was facilitated by high-level eutrophication and favorable environmental conditions. Furthermore, six potential germplasm sources of *U. prolifera* are summarized. The dominance of *Ulva* in the intertidal zone often indicates high eutrophication and deteriorating ecological conditions. With long-term reclamation and repeated ecological restoration projects, the intertidal vegetation is subjected to a vicious cycle of growth and destruction. Therefore, it is important to recognize that *U. prolifera* germplasm (macroalgae and micropropagules) will persist over the long term, and mudflats with monotonous and eutrophic habitats are highly likely to experience future large-scale algal blooms. Notably, a small-scale floating green tide was observed in the sea area near NETF in July 2023, and such concerns are not unfounded. This study conducts foundational scientific research on the attached green tide algae, a type of research that is relatively scarce in other marine areas. Most studies tend to initiate foundational research only after the outbreak of green tides, lacking early background data from the marine environment, thus rendering this study of significant reference value. Concurrently, this study emphasizes that field surveys remain an essential approach for conducting foundational scientific research on green tide algae in the NETF region, with the need to select appropriate research methods based

on the occurrence and development of algal mats, as required by the situation. Importantly, this study reflects the stability of marine ecosystems as a prerequisite for modern ocean management and services, provides new perspectives on the occurrence and development of green tides, and highlights potential ecological risk factors that should be considered in the implementation of intertidal construction projects.

KEYWORDS

ecological risk, harmful algal bloom, indicator species, ecosystem stability, reclamation, eutrophication, anthropogenic stressors, modern ocean management

1 Introduction

Coastal wetlands are a crucial component of the aquatic ecosystem, serving as a vital link between the ocean, freshwater, and land while providing unique ecological functions (Xu et al., 2024; Levin et al., 2001). They offer food and habitat for diverse ecosystems, and play a critical role in shoreline protection, mitigation of wind and wave impact, pollution control, maintenance of fishery resources, and promotion of carbon sequestration (Barbier et al., 2011; Mcleod et al., 2011). Additionally, wetlands hold significant value for educational, recreational, and tourism purposes (Barbier et al., 2011). The Nanhui-east-tidal-flat (NETF), situated in the southeast of Shanghai between the southern passage of the Yangtze River Estuary and Hangzhou Bay to the south (Figure 1), represents the largest marginal shoal in the Yangtze River Estuary area (Wei et al., 2017). Tides at this location are predominantly semi-diurnal. Positioned on the southern edge of the subtropical zone exposes NETF to the East Asian Monsoon climate.

The intertidal area of the NETF plays a crucial role in providing ecological services, serving as habitat and feeding grounds for intertidal creatures, as well as being an essential resting place for migratory birds along the East Asian–Australasian Flyway (Ge et al., 2007). Various species of vegetation are distributed across the intertidal gradient (Fan et al., 2006; You et al., 2018). *Phragmites australis* and *Spartina alterniflora* dominate the high tide zone, with *S. alterniflora* extending to the upper middle tide zone where it coexists with *Scirpus mariqueter*. The lower middle tide zone is characterized by different salt marsh pioneer species, followed by a bare mudflat. Notably, there are no higher plants present in the low tide zone (Fan et al., 2006; You et al., 2018).

Due to the rapid global population growth and accelerated urbanization, estuaries and coastal wetlands worldwide have suffered varying degrees of loss and degradation (Kennish, 2002; Crain et al., 2009; Barbier et al., 2011; Peter et al., 2024). From 1985 to 2010, a total of 754,697 hectares (ha) of coastal wetlands in China were reclaimed. Shanghai has reclaimed a total of 58,038.8 ha of tidal flats (Tian et al., 2016). The NETF is a post-reclamation mudflat wetland (Figure 1). Before reclamation, it was a nearshore marine ecosystem rather than an intertidal ecosystem. It has now become one of the most significant wetlands in the Yangtze River Estuary area.

The Yangtze River Estuary, the largest estuary system in Asia, is facing significant ecological stress due to a variety of human activities (Wei et al., 2015, 2017; Mei et al., 2018). The development of Shanghai has heavily relied on the natural land resources provided by the estuary (Yang, 2017), with river-driven deposition processes contributing to the expansion of tidal flat land (Figure 1). However, the construction of water conservancy facilities like the Three Gorges Dam has resulted in reduced sediment transport from the Yangtze River (Yang et al., 2011), leading to a slowdown in land deposition near the estuary. In addition to other factors such as rising sea levels and land erosion, the land deposition process near the NETF has slowed down (Wei et al., 2015). Combined with the reclamation projects following urbanization in Shanghai (Figure 1), by 2012, the tidal flats above 0 m in the NETF decreased by 80.8% (Wei et al., 2015). Additionally, reclamation activities have altered vegetation distribution (Han et al., 2010; Tao et al., 2017), zooplankton community composition (Li et al., 2012), waterbird diversity (Zhang, 2012; Niu et al., 2013), and benthic fauna composition (Ma, 2015; Yang, 2017) within the NETF ecosystem. Limited information regarding macroalgal proliferation in this region has been documented.

Marine vegetation, including macroalgae, plays a significant role in carbon sequestration (Liu et al., 2024a), contributing to approximately 50% of the burial of marine sediment carbon while occupying only 0.2% of the ocean area (Duarte et al., 2013; Krause-Jensen and Duarte, 2016). As one of the dominant primary producers in coastal ecosystems, macroalgae cover an area of about 3.5 million km^2 with a global net primary production of 1,521 TgC/yr (Krause-Jensen and Duarte, 2016). Additionally, macroalgae have the potential to mitigate climate change by absorbing CO_2, and their biomass is considered a sustainable feedstock for green energy and other types of blue carbon

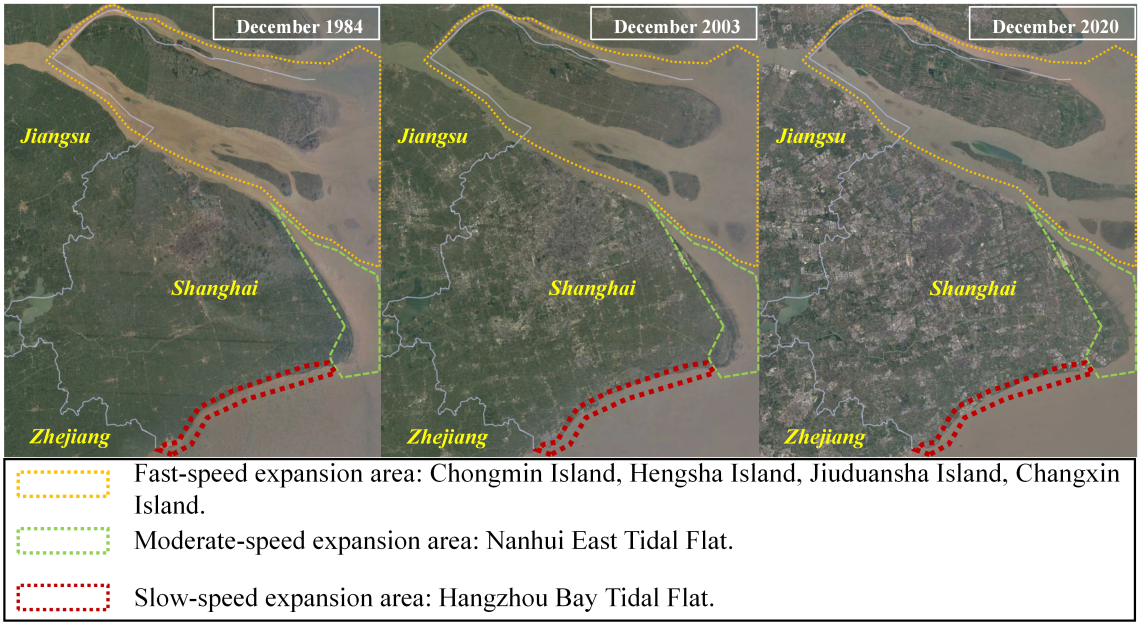

FIGURE 1
Satellite remote sensing imagery captured the expansion of Shanghai's urban area from 1984 to 2020, with data obtained from Google Earth Engine in April 2024. The significant increase in area in the Nanhui-east-tidal-flat occurred primarily between 2002 and 2003, as a result of Shanghai's utilization of land reclamation for the development of a modern coastal satellite city.

economy development (Yong et al., 2022). Chlorophyta (green seaweed) is a group of macroalgae. *Ulva* spp., an important green algae species (Shimada et al., 2008), has been utilized as an indicator of regional eutrophication and heavy metal pollution (Fort et al., 2020; Rybak, 2021; AbouGabal et al., 2023). *Ulva* possesses high nutritional value and is consumed by coastal residents in Asian countries (Sun et al., 2022b). It also serves as a natural source of polysaccharides and holds potential for use as antioxidants in the pharmaceutical industry (Farasat et al., 2014; Raposo et al., 2015; Bodar et al., 2024). However, large-scale blooms of *Ulva* have been occurring along the coast of China (Liu et al., 2013a; Liu et al., 2021a, 2022; Sun et al., 2022a; Xia et al., 2022a, 2024a; Feng et al., 2024; He et al., 2023). Therefore, studying the distribution and species proliferation of green macroalgae is crucial.

The current study investigated the spatial distribution and biomass of green seaweeds in the NETF, utilizing a combination of morphological and molecular biological methods to assess their taxonomic species. Additionally, environmental factors such as sea surface temperature (SST), sea surface salinity (SSS), pH, dissolved oxygen, chemical oxygen demand, inorganic nitrogen, active phosphate, petroleum, and other parameters were analyzed for further analysis and discussion. Overall, this research examines the taxonomy, spatial patterns, and variability of macroalgae in the NETF while also evaluating the potential for future large-scale green tide outbreaks in relation to environmental factors. So far, the occurrence of a small-scale floating green tide near the NETF in 2023 has been observed. The implication of attached green seaweeds in this region is underscored, along with a preliminary ecological risk assessment. This also provides foundational data and guidance for monitoring protocols for subsequent long-term surveillance.

2 Materials and methods

2.1 Distribution of green seaweeds in the NETF

The distribution and species identity of green seaweeds along the coastline of the NETF were systematically investigated from March to May 2021. A Global Positioning System (GPS) was utilized to accurately record the precise geographical coordinates of the green seaweed distribution (Figure 2). Specimens of green seaweeds were meticulously collected, and their respective habitats and types of solid substratum were thoroughly documented. Green seaweeds were observed at designated stations A-H (Figure 2A), with stations A-E forming part of the transect line (Figures 2B, C). The sampling sites were delineated using Surfer 16.0 software (Golden Software, Colorado, USA).

2.2 Green seaweed biomass and dry-wet ratio

Field surveys were conducted in accordance with the "The specification for marine monitoring, Part 7: Ecological survey for offshore pollution and biological monitoring" (National Standard of the People's Republic of China, GB17378.7-2007). Green seaweeds were collected on March 12, March 18, March 27, April 4, April 13, and May 1 of 2021 based on their distribution as described in Section 2.1 and sampling availability. The biomass of green seaweeds was measured at points A, B, C, D, and E along a line transect arranged in the intertidal zone (line transect, Figure 2), with a sampling point set

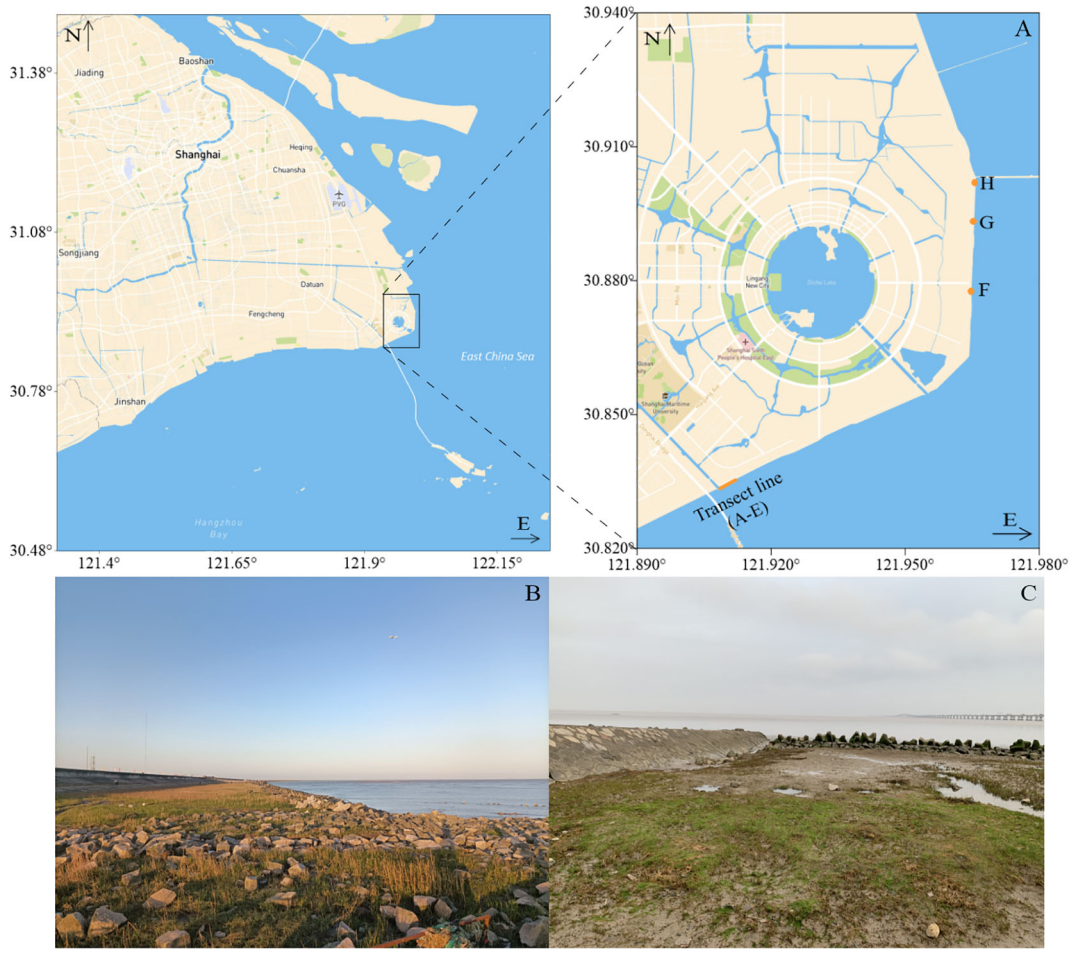

FIGURE 2
(A) Eight sampling sites (stations A-H) were selected, with transect lines consisting of five equally spaced sampling points (stations A-E); **(B)** The habitat characteristics along the transect line were documented; **(C)** The distribution of green seaweed at point E in the transect line revealed attached populations throughout the green areas.

every 250 m. Samples were collected using a quadrat measuring 0.25 m × 0.25 m and immediately transported to the laboratory under cool conditions. Fresh green seaweeds were carefully cleaned of adhering sediment with a brush and dried using an electric thermostatic drying oven until reaching constant weight (Shanghai Yiheng Scientific Instrument Co., Ltd., Shanghai, China). The wet weight (WW) and dry weight (DW) of the seaweeds were measured using an electronic balance (AL-104, Mettler Toledo, Zurich, Switzerland). Origin 2019b (OriginLab, Massachusetts, USA) software was used to plot biomass and dry-wet ratio curves. GraphPad Prism 9 (version 9.5.1) was used for variance analysis. Algal biomass was expressed as mean ± standard deviation (X ± SD).

2.3 Morphology and molecular identification of green seaweeds

The green seaweeds collected were initially classified based on their morphology, and the micro-morphology was observed and photographed using an optical microscope (E200, Nikon, Tokyo, Japan). Three to eight strains of green seaweeds were selected from each station, A-H. Prior to molecular identification, the surface sediment and other impurities were removed by brushing. The Dzup (Plant) genomic DNA isolation reagent (B518203-0025, Sangon Bioengineering Co., Ltd., Shanghai) was utilized for DNA extraction. The internal transcribed spacer (ITS) and 5S ribosomal DNA (5S) primers were utilized for the identification of *Ulva* algae (Liu et al., 2022; Zhao et al., 2023). The polymerase chain reaction (PCR) cycling conditions followed those described by Liu et al. (2022). The PCR reaction mixture consisted of 50 μL, comprising 25 μL of 2× PCR-mix, 19 μL of dd-H_2O, 2 μL (10 mM) of each forward and reverse primers, and 2 μL of DNA template. Amplification was carried out using a PCR machine (Thermo Fisher Scientific, Singapore). Following confirmation via electrophoresis on a 1% gel, the qualified PCR products were submitted to Sangon Bioengineering (Shanghai) Co., Ltd. for Sanger sequencing.

The obtained sequences were corrected using Chromas 2.3 software, which included 31 ITS sequences and 31 5S sequences. Subsequently, the sequences were compared using the Basic Local Alignment Search Tool (BLAST) within the National Center for Biotechnology Information (NCBI, https://www.ncbi.nlm.nih.gov/) to further identify the specific species of macroalgae. The ITS

sequences of similar *Ulva* species, including *U. prolifera*, *Ulva linza*, *Ulva compressa*, and *Ulva flexuosa*, were then downloaded from the NCBI database for comparison. *Blidingia minima* was selected as the outgroup and the 5S sequence of *U. linza* was chosen for further study. Detailed sample information can be found in Table 1.

2.4 Phylogenetic tree construction and genetic diversity analysis

The sequences were aligned using MEGA X software (Kumar et al., 2018), and a maximum likelihood (ML) phylogenetic tree was constructed based on the Kimura two-parameter model (Kimura, 1980). Genetic distances were calculated, and the reliability of each branch was verified through 1,000 bootstrap tests. The constructed trees were further enhanced using the iTOL database (https://itol.embl.de/) (Letunic and Bork, 2021). All 62 sequences have been deposited in the NCBI database (Table 1).

2.5 Data collection and statistical analysis of environmental factors

Data for SST and SSS in the NETF from January 1 to December 31 of 2021 were acquired from the National Marine Data Center of China, while data on pH, dissolved oxygen, chemical oxygen demand, inorganic nitrogen, active phosphate, and petroleum in the NETF from May 2017 to March 2023 were obtained from the Online Water Quality Monitoring System. Seawater quality categories were determined based on the "Seawater Quality Standard" (Ministry of Ecology and Environment of the People's Republic of China, GB 3097-1997). The standard applies to the maritime jurisdiction of China and adopts the single-factor method for assessing seawater quality. According to the standard, seawater quality is categorized into five levels, ranging from high to low: Grade I (excellent water quality: suitable for marine fisheries, marine nature reserves, and reserves for rare and endangered marine life; evaluation criteria include: pH range of 7.8 to 8.5 with a permissible normal fluctuation not exceeding 0.2, $C_{(Dissolved\ Oxygen)} \geq 6$ mg/L, $C_{(Chemical\ Oxygen\ Demand)} \leq 2$ mg/L, $C_{(inorganic\ nitrogen)} \leq 0.20$ mg/L, $C_{(Active\ phosphate)} \leq 0.015$ mg/L, $C_{(Petroleum)} \leq 0.05$ mg/L, etc.), Grade II (good water quality: suitable for aquaculture areas, bathing areas, marine sports or recreational areas with direct human contact with seawater, and industrial water areas directly related to human consumption; evaluation criteria include: pH range of 7.8 to 8.5 with a permissible normal fluctuation not exceeding 0.2, 5 mg/L $\leq C_{(Dissolved\ Oxygen)} <$ 6 mg/L, 2 mg/L$< C_{(Chemical\ Oxygen\ Demand)} \leq$ 3 mg/L, 0.20 mg/L$< C_{(inorganic\ nitrogen)} \leq$ 0.30 mg/L, 0.015 mg/L$< C_{(Active\ phosphate)} \leq$ 0.030 mg/L, $C_{(Petroleum)} \leq$0.05 mg/L, etc.), Grade III (ordinary water quality: suitable for general industrial water areas and coastal scenic tourism areas; evaluation criteria include: pH range of 6.8 to 8.8 with a permissible normal fluctuation not exceeding 0.5, 4 mg/L $\leq C_{(Dissolved\ Oxygen)} <$ 5 mg/L, 3 mg/L$< C_{(Chemical\ Oxygen\ Demand)} \leq$ 4 mg/L, 0.30 mg/L$< C_{(inorganic\ nitrogen)} \leq$ 0.40 mg/L, 0.015 mg/L$< C_{(Active\ phosphate)} \leq$ 0.030 mg/L, 0.05 mg/L$< C_{(Petroleum)} \leq$ 0.30 mg/L, etc.), Grade IV (deviant water quality: suitable for marine port waters and marine development and operational areas; evaluation criteria include: pH range of 6.8 to 8.8 with a permissible normal fluctuation not exceeding 0.5, 3 mg/L $\leq C_{(Dissolved\ Oxygen)} <$ 4 mg/L, 4 mg/L$< C_{(Chemical\ Oxygen\ Demand)} \leq$ 5 mg/L, 0.40 mg/L$< C_{(inorganic\ nitrogen)} \leq$ 0.50 mg/L, 0.030 mg/L$< C_{(Active\ phosphate)} \leq$ 0.045 mg/L, 0.30 mg/L$< C_{(Petroleum)} \leq$ 0.50 mg/L, etc.), and Worse than Grade IV (extremely poor water quality: seawater quality is worse than the above four categories).

The environmental data was analyzed using Microsoft Excel (Excel 2016, Microsoft, Washington, USA). The eutrophication level in the NETF was evaluated using the eutrophication index method. The calculation formula for the eutrophication index is as follows (1):

$$E = C_{(Chemical\ Oxygen\ Demand)} \times C_{(Inorganic\ Nitrogen)} \times C_{(Active\ phosphate)} \times 10^6/4500 \quad (1)$$

where E represents the eutrophication index and C represents the concentration (mg/L). When $1 \leq E \leq 3$, eutrophication is classified as mild; when $3< E \leq 9$, it is classified as medium; and when $E > 9$, it is classified as heavy (Liu et al., 2024b). Additionally, Origin 2019b and Surfer 9 software were employed for data analysis, figure drawing, and assembly.

3 Results

3.1 Vegetation distribution and solid substrate types of green seaweeds in the NETF

During the spring of 2021, green seaweeds were collected from eight designated stations (stations A-H) along the coastline of the NETF, primarily in the intertidal zone with relatively gentle terrain slopes. Stations A-E exhibited a dominance of *S. alterniflora* and *P. australis* among higher plants, with sporadic occurrences of *S. mariqueter*. Four types of solid substrates were identified at stations A-E, including discarded fishing nets, woven bags, and bottles (Figure 3A); hard materials such as crushed stones, broken bricks, and artificial dams (Figure 3B); residual roots from withered higher plants or roots of new plants (Figure 3C); as well as sediment (Figure 3D). In contrast, stations F-G presented a relatively simple habitat where *S. alterniflora* dominated among higher plants. The green seaweeds were mainly dispersed across the mudflat.

3.2 Morphology, molecular identification, and genetic diversity

The samples collected from the NETF exhibited a dark green or bright green coloration (Figure 4A) and were initially identified as *Ulva* spp. The seaweeds displayed numerous branches and an anchorage structure, with wide blades primarily consisting of primary branches and few secondary branches (Figure 4A). During the growth period, the seaweeds in the intertidal zone of the NETF appeared to have developed conspicuous air bladders (Figure 4B). The cells were arranged irregularly in monolayers,

10.3389/fmars.2025.1505586

TABLE 1 Detailed information about the macroalgae used to build the phylogenetic tree.

Species Number	Authority	Collection Locality	GenBank Information (ITS)	GenBank Information (5S)	Source	Specimen Location	Reference
2021ESNHA1, 2021ESNHA2, 2021ESNHA3	This study	East China Sea, China	OR543030, OR543031, OR543032	OR544859, OR544860, OR544861	This study	Shanghai Ocean University	This study
2021ESNHB1, 2021ESNHB2, 2021ESNHB3	This study	East China Sea, China	OR543033, OR543034, OR543035	OR544862, OR544863, OR544864	This study	Shanghai Ocean University	This study
2021ESNHC1, 2021ESNHC2, 2021ESNHC3	This study	East China Sea, China	OR543036, OR543037, OR543038	OR544865, OR544866, OR544867	This study	Shanghai Ocean University	This study
2021ESNHD1, 2021ESNHD2, 2021ESNHD3	This study	East China Sea, China	OR543039, OR543040, OR543041	OR544868, OR544869, OR544870	This study	Shanghai Ocean University	This study
2021ESNHE1, 2021ESNHE2, 2021ESNHE3	This study	East China Sea, China	OR543042, OR543043, OR543044	OR544871, OR544872, OR544873	This study	Shanghai Ocean University	This study
2021ESNHH1, 2021ESNHH2, 2021ESNHH3, 2021ESNHH4, 2021ESNHH5, 2021ESNHH6, 2021ESNHH7, 2021ESNHH8	This study	East China Sea, China	OR543045, OR543046, OR543047, OR543048, OR543049, OR543050, OR543051, OR543052	OR544874, OR544875, OR544876, OR544877, OR544878, OR544879, OR544880, OR544881	This study	Shanghai Ocean University	This study
2021ESNHF1, 2021ESNHF2, 2021ESNHF3, 2021ESNHF4, 2021ESNHF5	This study	East China Sea, China	OR543053, OR543054, OR543055, OR543056, OR543057	OR544882, OR544883, OR544884, OR544885, OR544886	This study	Shanghai Ocean University	This study
2021ESNHG1, 2021ESNHG2, 2021ESNHG3	This study	East China Sea, China	OR543058, OR543059, OR543060	OR544887, OR544888, OR544889	This study	Shanghai Ocean University	This study
6XSG-6	*Ulva prolifera*	Xiangshan Bay, Zhejiang province, China	KT802966	KT803042	NCBI	Institute of Oceanology, Chinese Academy of Sciences	(Zhang et al., 2018)
SDA4	*Ulva linza*	Zhanqiao, Qingdao, China	HM584731	HM584773	NCBI	Ningbo Entry-Exit Inspection and Quarantine Bureau Technical Center	(Duan et al., 2012)
SDF12	*Ulva compressa*	Jinshatan, Qingdao, China	HM584738	N.A.	NCBI	Ningbo Entry-Exit Inspection and Quarantine Bureau Technical Center	(Duan et al., 2012)
4X-1	*Ulva flexuosa*	Xiaoyangkou, Subei Shoal, China	KT802910	N.A.	NCBI	Institute of Oceanology, Chinese Academy of Sciences	(Zhang et al., 2018)
MurDG	*Blidingia minima*	Muroran D (Charatsunai), southern Hokkaido, Japan	AF163104	N.A.	NCBI	University of New South Wales	(Woolcott et al., 2000)

N.A., no information.

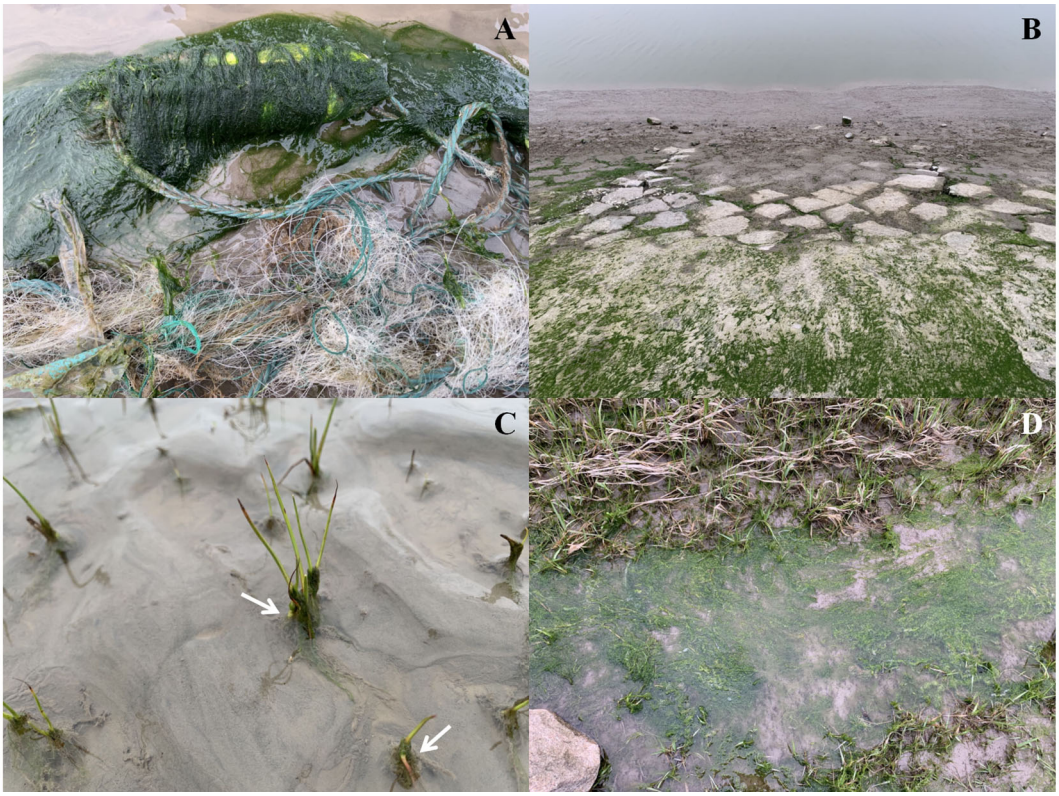

FIGURE 3
Main solid substrate types of green seaweeds in the Nanhui-east-tidal-flat. **(A)** Plastic waste, **(B)** Natural or artificial reef, **(C)** Intertidal plant roots (white arrows), and **(D)** Sediment.

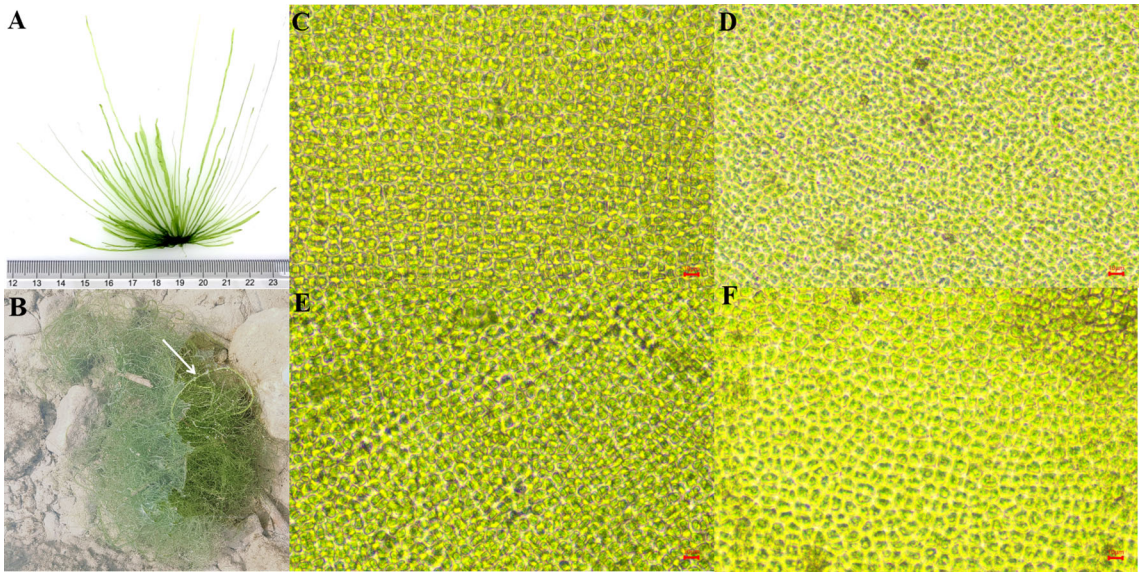

FIGURE 4
(A) The morphology of green seaweeds in the Nanhui-east-tidal-flat; **(B)** The air bladders of the seaweeds (white arrows); **(C)** The cell morphology of seaweeds in the transect line; **(D-F)** The cell morphology of seaweeds at stations F-H.

being oval or polygonal in shape (Figures 4C–F). Based on ITS and 5S sequences, BLAST results indicated that the 31 samples shared more than 98% similarity with *U. prolifera*. Two phylogenetic trees were constructed for further confirmation of the species.

The ML tree constructed based on the ITS revealed that 36 sequences, including outgroups, were clustered into four branches, and 31 samples from the NETF were distinguished from *U. compressa* (HM584738) and *U. flexuosa* (KT802910). However, these 31 samples were grouped into the *U. linza-procera-prolifera* complex group (LPP) with *U. prolifera* (KT802966) and *U. linza* (HM584731) (Figure 5), indicating that the ITS could not distinguish between *U. prolifera* and *U. linza* effectively. Therefore, it is recommended to use the 5S region for better resolution. The ML tree constructed based on the 5S region showed that all 31 samples from NETF formed a main clade with *U. prolifera*, suggesting that they indeed all belong to this species (Figure 6).

3.3 Variation of green macroalgal biomass in the NETF

Overall, the biomass (WW and DW) of attached *U. prolifera* in the NETF exhibited an increasing trend from March to May 2021 (Figure 7). The WW of *U. prolifera* on March 12, March 18, March 27, April 4, April 13, and May 1 of 2021 was measured at 85.9301 ± 30.1555 g/m^2, 96.7104 ± 38.4215 g/m^2, 114.9303 ± 72.7708 g/m^2, 223.8895 ± 124.3791 g/m^2, 225.0913 ± 89.5540 g/m^2, and 373.6229 ± 208.0184 g/m^2, respectively (Figure 7). The DW of *U. prolifera* on March 12, March 18, March 27, April 4, April 13, and May 1 of 2021 measured 11.0117 ± 1.8634 g/m^2, 11.7029 ± 2.4305 g/m^2, 12.6385 ± 6.3048 g/m^2, 27.6035 ± 17.6919 g/m^2, 33.1949 ± 16.4219 g/m^2, and 72.7904 ± 48.1359 g/m^2, respectively (Figure 7). The high SD of *U. prolifera* biomass at various stations on March 27, April 4, April 13, and May 1 of 2021 (Figure 7) was attributed to the heterogeneous distribution of *U. prolifera* in the intertidal zone. As environmental conditions gradually warmed, they became more conducive to the germination and growth of *U. prolifera*. The attached *U. prolifera* in the NETF exhibited continuous growth from March to May of 2021, with an increasing trend in average biomass (Figure 7), reaching 373.6229 g/m^2 (WW) and 72.7904 g/m^2 (DW) on May 1, 2021. The water content of *U. prolifera* in the NETF ranged from 80.5177% to 89.0033% with an average of 86.2548%. Generally, the average water content of *U. prolifera* ranges from 75% to 96.6%, and that of *U. prolifera* collected in the present study fell within this range.

3.4 Assessment of the environmental factors, seawater quality categories, and eutrophication level of the NETF

The annual SST in the NETF ranged from 5.2°C to 29.1°C (Figure 8A). *Ulva prolifera* is capable of year-round survival within

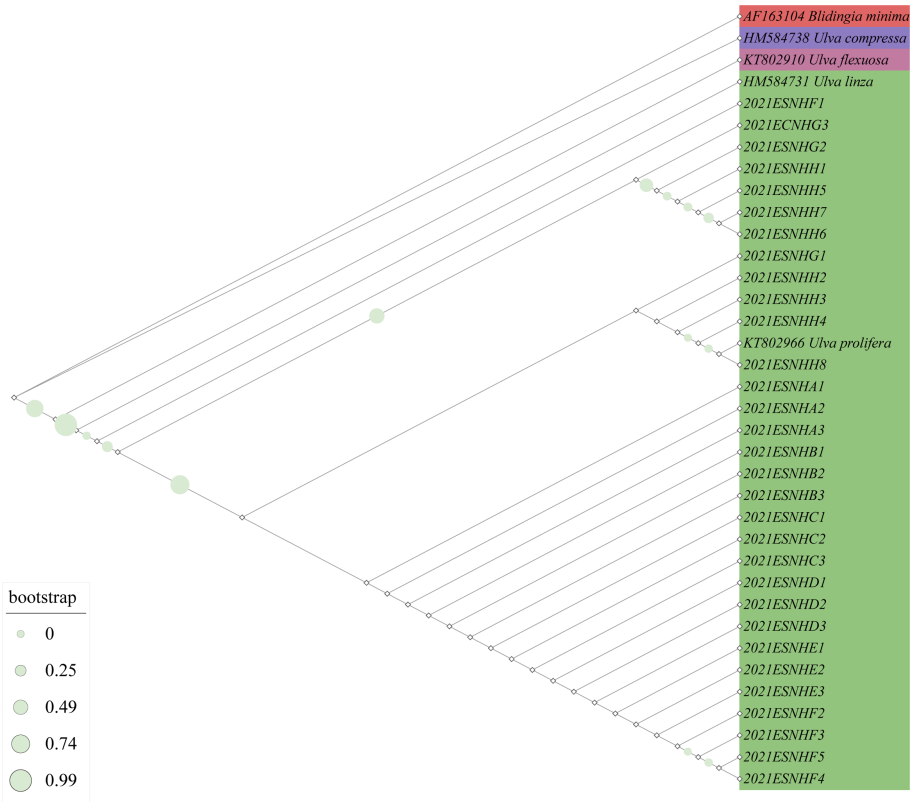

FIGURE 5
Maximum likelihood phylogenetic tree constructed based on ITS sequences.

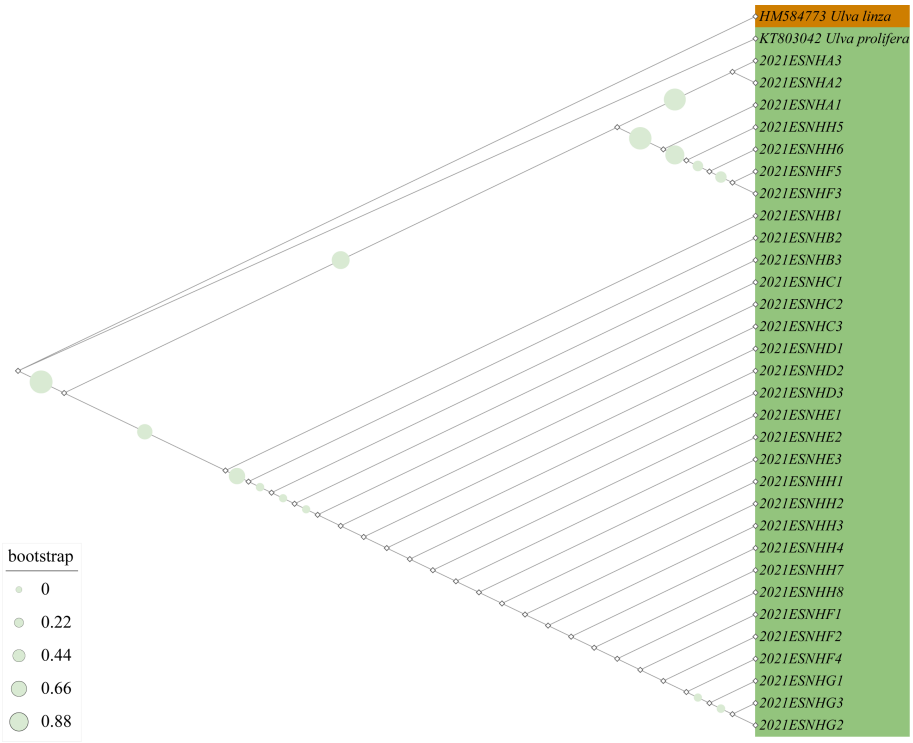

FIGURE 6
Maximum likelihood phylogenetic tree constructed based on 5S sequences.

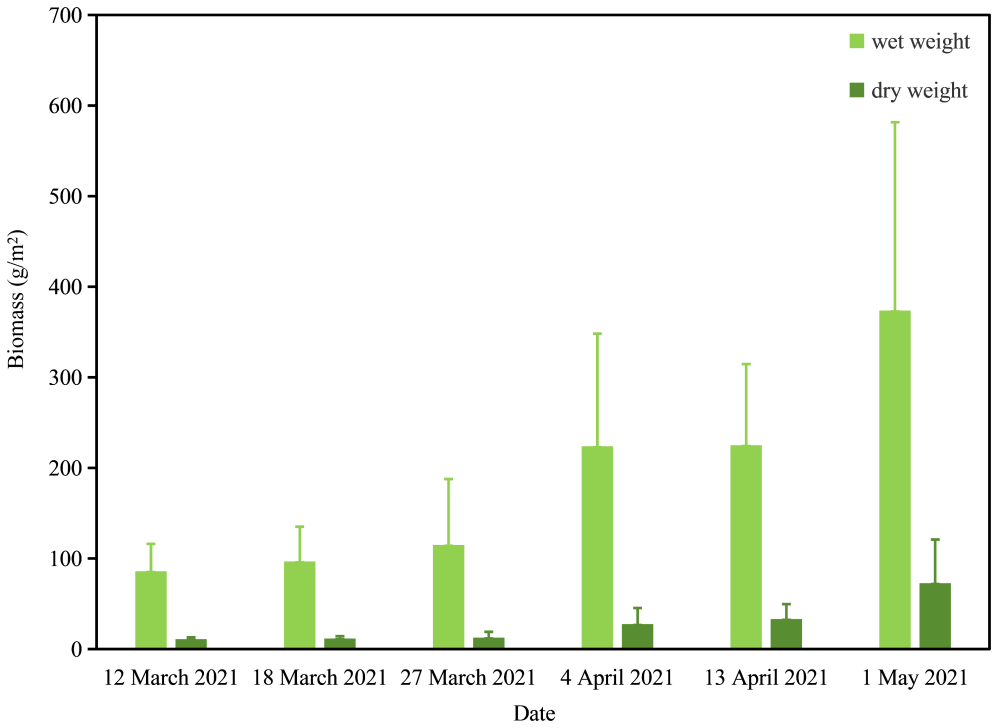

FIGURE 7
The wet and dry weights of attached *U. prolifera* in the NETF from March to May 2021.

this temperature range (Xiao et al., 2016). In the Northern Hemisphere, the SSTs of the NETF in March, April, and May ranged from 9.5°C to 13.4°C, 12.5°C to 17.2°C, and 17.1°C to 21.3°C, respectively. The monthly average SST in March, April, and May measured at about 10.98°C, 14.68°C, and 19.60°C, respectively. Previous studies have indicated that *U. prolifera*'s daily growth rate was highest at temperatures between 15°C and 25°C. The SST in April and May within the NETF was evidently conducive for the growth and biomass accumulation of *U. prolifera* (Figure 7; Figure 8A). In comparison with March and April, the temperature conditions in May were more favorable for *U. prolifera*'s growth. During the monitoring period, the WW and DW of *U. prolifera* per unit area within the NETF reached their peak levels in May (Figure 7).

The annual SSS in the NETF ranged from 12 psu to 27.5 psu (Figure 8B). Despite significant seasonal fluctuations, *U. prolifera* can survive year-round within this range of salinity (Rybak, 2018). The ranges of SSS in the NETF during March, April, and May were 21.8 psu to 24.7 psu, 21.9 psu to 22.1 psu, and 13.9 psu to 19.9 psu, respectively. The monthly average SSSs in March, April, and May were calculated as about 22.87 psu, 22.01 psu, and 16.30 psu, respectively. The SSS of the NETF provides a suitable environment for the growth of *U. prolifera* (Xiao et al., 2016; Li et al., 2017).

The pH at the NETF ranged from 7.79 to 8.12 (Figure 9A) between May 2017 and March 2023, with a monthly average of 7.99, indicating suitable conditions for the growth of *U. prolifera* (Li et al., 2017). The $C_{(Dissolved\ Oxygen)}$ in the NETF ranged from 5.58 mg/L to 8.86 mg/L (Figure 9B), with an average value of 7.63 mg/L. The $C_{(Chemical\ Oxygen\ Demand)}$ ranged from 1.18 mg/L to 3.66 mg/L (Figure 9C), averaging at 2.42 mg/L. The $C_{(Inorganic\ Nitrogen)}$ ranged from 0.377 mg/L to 1.527 mg/L (Figure 9D), with an average value of 0.98 mg/L. The $C_{(Active\ phosphate)}$ ranged from 0.017 mg/L to 0.064 mg/L (Figure 9E), with an average value of 0.04 mg/L, indicating a general declining trend (Figure 9E). The $C_{(Petroleum)}$ ranged from 0 mg/L to 0.051 mg/L (Figure 9F), with an average value of 0.02 mg/L, showing an initial increase followed by a decrease (Figure 9F). Based on these six monitoring indexes, the single factor method identified the seawater quality of the NETF as predominantly Worse than Grade IV (Figure 10). With only Grade III and Grade IV identified in August 2022 and October of 2022 respectively, the seawater quality has been persistently poor for an extended period.

From May 2017 to March 2023, the NETF exhibited significant eutrophication, with E values ranging from about 3.38 to 58.82 and an average of about 25.04. Only in August 2022 was the E value<9 (about 3.38), indicating medium eutrophication. During all other monitoring periods, the E values exceeded 9, indicating heavy eutrophication. For instance, in April 2021, the E value of the NETF was recorded at about 21.26. The presence of seawaters with heavy or medium eutrophication (Figures 9, 10) provided ample nutritional support for *U. prolifera* in the intertidal zone (Figures 2, 3), resulting in its high biomass per unit area within the NETF (Figure 7).

4 Discussion

4.1 Implications of *Ulva* morphology and biodiversity in the NETF

Macroalgae plays a crucial role as habitat-forming organisms in coastal ecosystems of temperate and subtropical regions (Graba-Landry et al., 2018). The genus *Ulva* L. (Ulvales) is widely

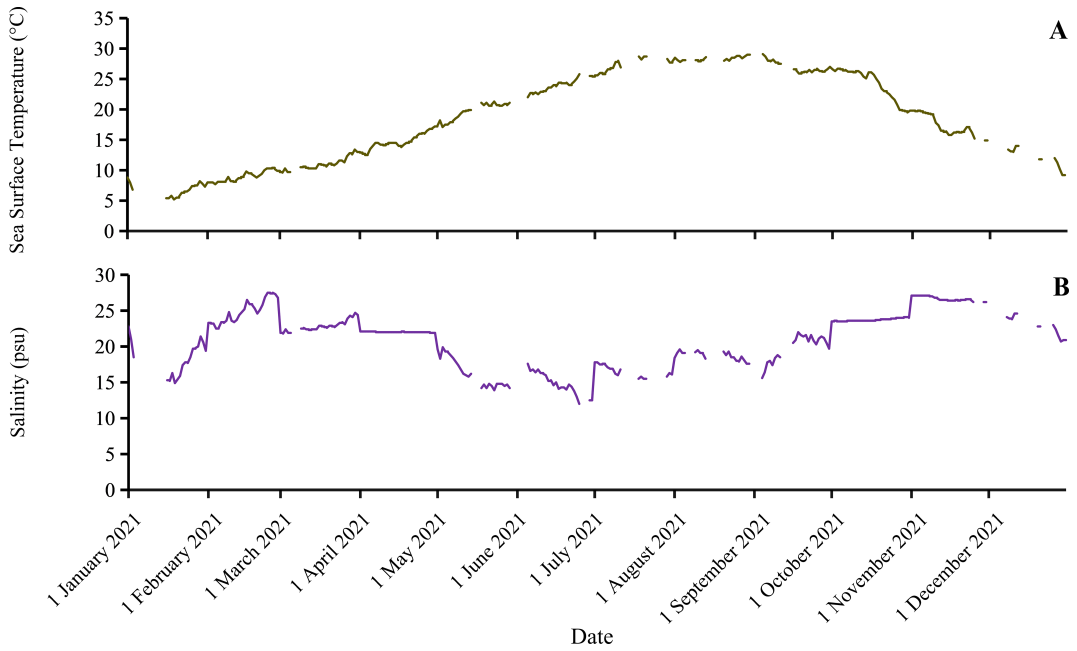

FIGURE 8
Data of sea surface temperature **(A)** and salinity **(B)** in the sea area of the NETF.

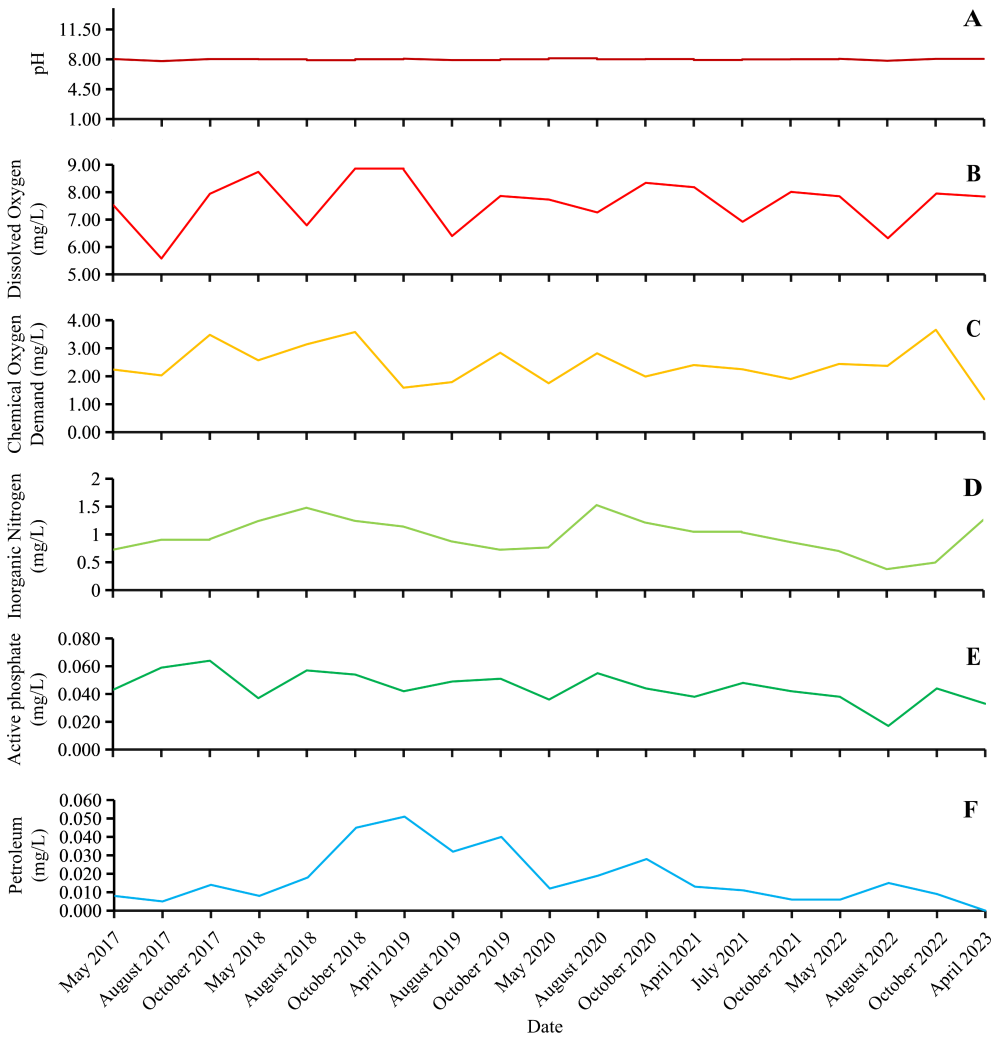

FIGURE 9
Data of pH **(A)**, $C_{(Dissolved\ Oxygen)}$ **(B)**, $C_{(Chemical\ Oxygen\ Demand)}$ **(C)**, $C_{(Inorganic\ Nitrogen)}$ **(D)**, $C_{(Active\ phosphate)}$ **(E)**, and $C_{(Petroleum)}$ **(F)** in the sea area of the NETF.

distributed worldwide, primarily inhabiting estuaries, intertidal zones, and other coastal areas. Species such as *Ulva pertusa* (Chen et al., 2022), *Ulva lactuca* (Human et al., 2016) and *U. prolifera* (Li et al., 2024a; Sun et al., 2022b), *Ulva rigida* (Dartois et al., 2021), and other macroalgae are commonly found in intertidal zones. The NETF is an important wetland in the Yangtze River Estuary area, rich in biological resources. However, the morphology of *U. prolifera* collected in this study appears to be atypical (Figure 4A), possibly influenced by unique environmental factors present on the intertidal mudflat. The morphology of *Ulva* spp. can be influenced by various factors including thallus age, lifestyle (Loughnane et al., 2008; Wolf et al., 2012), microbiology (Wichard, 2015; Chen, 2018; Alsufyani et al., 2020), environmental temperature (Gao et al., 2016), light intensity (Wu et al., 2022), salinity (Gao et al., 2016), nutrient concentration (Blomster et al., 2002), among others. Compared with the floating populations of *U. prolifera* from the green tide in the southern Yellow Sea, the blades of the attached *U. prolifera* collected in this study exhibited greater width and fewer secondary branches. The observed disparity in branching phenotypes may be attributed to the two distinct ecotypes of *U. prolifera* (i.e., attached and floating ecotypes) (Ma et al., 2020).

Environmental factors and volatility in the intertidal zone of the NETF (Figure 8B) may have also contributed to the differences in the morphology of *U. prolifera*. It has been found that at a suitable temperature and higher salinity (from 20 psu to 30 psu), the branches of *U. prolifera* were reduced, and the thalli were wider and well-dispersed (Gao et al., 2016). During the investigation, the salinity of NETF was around 22. The tendency for *U. prolifera* thalli to be leaf-like was similarly observed (Figure 4A). Such morphology facilitates *U. prolifera* to reduce shading, obtain sufficient light and nutrients to maintain high growth rates (Gao et al., 2016), and dominate in complex intertidal habitats. Due to this plasticity in morphological traits (Wichard et al., 2015; Gao et al., 2016), some *Ulva* spp. can often adapt to the variable and harsh environments of the intertidal zone (Innes, 1988).

The morphological variations of the green macroalgae in the genus *Ulva* present significant challenges for traditional morphological identification (Hayden et al., 2003). DNA barcoding

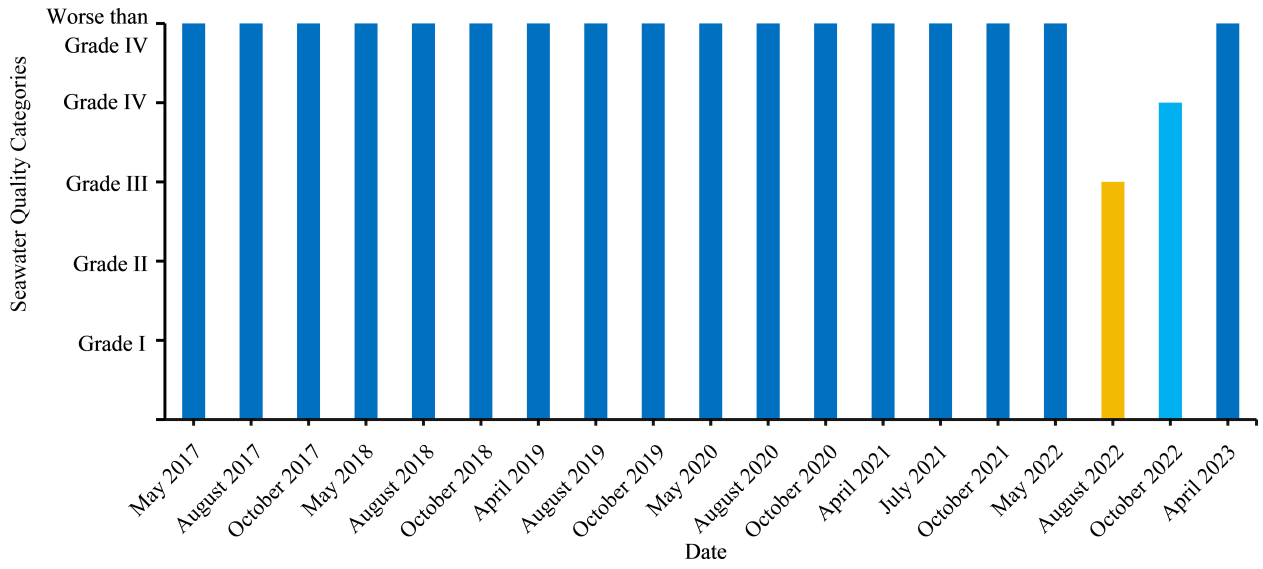

FIGURE 10
Data of seawater quality categories in the sea area of the NETF.

technology has been recognized as an effective approach to the identification of green macroalgae (Du et al., 2014). The combination of ITS + 5S primers identified all the green macroalgae collected in this study as *U. prolifera*, indicating that a single dominant species was prevalent among the green macroalgae distributed in the NETF during spring 2021. Consequently, there was a low biodiversity of green macroalgae in the NETF and relatively simple trophic pathways within this intertidal environment (Riera et al., 2004). Furthermore, being an artificial habitat, the NETF may exhibit lower ecosystem resilience and stability.

4.2 Potential factors influencing the distribution of green macroalgae in the NETF

Due to the significant longitudinal gradient in environmental and biological factors within the intertidal zone, spatial zonation is observed in the population of macroalgae, resulting in low species diversity (Park and Hwang, 2011; Choi and Kim, 2004). For instance, *Ulva* spp. are typically dominant in temperate and subtropical intertidal mudflats (Park and Hwang, 2011; Sun et al., 2022b). The distribution of macroalgae in the intertidal mudflat will be influenced by a variety of environmental factors, including biological and physical elements. For instance, *Ulva* spp. are impacted by interspecific competition and predator behavior (Park and Hwang, 2011), with *Ampithoe* spp. exhibiting high abundance in the NETF (Li et al., 2023a) and playing a crucial role in controlling the biomass of *U. prolifera*. Physical factors encompass irradiance, temperature, nutrient level, tidal heights (Choi and Kim, 2004), and currents (de Guimaraens and Coutinho, 2000). Typhoons, for example, are frequent in the East China Sea, and their waves have adverse effects on the stability of intertidal zones in the NETF (Wang JY. et al., 2022; Chi et al., 2023; Li et al., 2024b). Original intertidal habitats may be destroyed and restoring biodiversity and siltation will necessitate prolonged biogeochemical processes. Furthermore, sediment dynamics and size affect the spatial distribution of *U. prolifera* (Park and Hwang, 2011). Park and Hwang (2011) identified a clear relationship between the density of *U. prolifera* and the ratio of sand to silt in the intertidal flats. Laboratory experiments also demonstrated a significant association between micropropagule survival and sandy sediment particle size.

The sediments of the NETF are primarily sourced from the Yangtze River, consisting mainly of silty sediment with a minor presence of clay. The clay minerals include illite, chlorite, and kaolinite (Yan et al., 2011; Xia et al., 2022b). Further investigation is needed to understand the specific factors influencing the distribution of *U. prolifera* on silty sediment. The construction of dykes and concrete breakwaters in the NETF has a wave-abatement effect, creating relatively calm seawater along the shoreline that provides a suitable habitat for *U. prolifera* and facilitates attachment and germination of its micropropagules. In addition to physical factors, it was observed that *U. prolifera* can persist and grow on decaying higher plants and their seedling roots (Figure 3C). Interestingly, *U. prolifera* exhibited limited distribution in the intertidal zone, characterized by dense growth of higher plants, indicating that the distribution of higher intertidal vegetation influences the spatial pattern of *U. prolifera*. This may be attributed to ecological niche differentiation resulting from interspecific competition, and further investigation into the distribution relationships and mechanisms between intertidal macroalgae and higher vegetation is warranted.

Eutrophication and global warming are significant factors influencing the distribution of macroalgae (Liu et al., 2021b; Qi et al., 2022). The East China Sea has been profoundly impacted by global climate change (Zhang WX. et al., 2022), particularly through an increasing trend in SST, which has implications for the stability of

the marine ecosystem. The increasing SST in China is mainly due to the change in the ocean circulation over the continental shelf caused by local atmospheric forcing (Sasaki and Umeda, 2021). Currently, the response of SST to global warming in China's offshore waters exceeds the global average increase in SST. Moreover, there has been a recent acceleration in the rate of warming over the past decade (Tang et al., 2020). Eutrophication is prevalent in the NETF sea area with heavy or moderate eutrophication observed (Figures 9, 10), and runoff from the Yangtze River significantly contributes to nutrient fluxes within both estuarine and offshore areas (Sun et al., 2023). Within the study area, numerous rivers flow into the East China Sea, discharging nutrient-rich water and creating favorable conditions for the growth and reproduction of macroalgae (*U. prolifera*) in the estuarine intertidal zone. The suitable marine climatic conditions in the mid-latitude region are the "cradle" and "hotbed" for the growth of *U. prolifera*, and environmental factors such as SST (Figure 8A), SSS (Figure 8B), and pH (Figure 9A) in the NETF satisfy the growth conditions of *U. prolifera* (Lin et al., 2011; Ichihara et al., 2013; Cui et al., 2015; Xiao et al., 2016; Rybak, 2018; Zhao et al., 2021). Therefore, the biomass of *U. prolifera* in the NETF has begun to take shape, as indicated by Figures 2, 3, 7. Gradually forming small-scale algal mats have been observed in the intertidal zone (Figures 2, 3).

Reclamation activities in Shanghai since 1953 have contributed to a roughly 20% expansion of the urban area (Wei et al., 2015). Over the past century, the NETF has undergone several projects aimed at promoting silt accumulation (Figure 1). For instance, from 2003 to 2006, approximately 133.3 km^2 of land was reclaimed in Shanghai, leading to an expansion of the coastline both eastward and southward through artificial construction (Figure 1), resulting in the destruction and eventual disappearance of the original intertidal habitat (Zhang, 2012). Subsequently, following natural succession and artificial ecological restoration, *P. australis*, *S. alterniflora*, *S. mariqueter* as well as small amounts of *Suaeda salsa* and *Suaeda glauca* were observed on the newly formed tidal flat (Zhao et al., 2024). In conjunction with the establishment of the Lin-gang Special Area of China (Shanghai) Pilot Free Trade Zone in 2019, there has been a significant alteration in the land-use pattern of the NETF and its environs, resulting from substantial anthropogenic disturbances. Commencing from March 2021 to May 2022, a new phase of slope renovation, roughening, and beach preservation activities was initiated on the outer slopes of the sea ponds at the NETF (Figure 11). Subsequently, in July 2022, the Shanghai Lin-gang Coastal Marine Ecological Protection and Restoration Project was officially inaugurated (Figure 11). Since 2021, researchers have encountered challenges conducting cyclical marine scientific research within the NETF due to ongoing engineering construction projects within this area. In particular, since June of 2021, the habitats in the sample area have been impacted by coastal engineering construction (Figure 11). Although there is still sporadic distribution of attached *U. prolifera* in the vicinity of the sample area, conducting standardized scientific research has become challenging. Once the marine ecological protection and restoration project (artificial modification of the intertidal zone) is completed and the NETF habitat has stabilized, it will be feasible to study *Ulva* spp. distribution in the NETF as well as species succession, aligning with natural evolutionary patterns. It is foreseeable that alterations to the shoreline may lead to changes in waves, currents, and a variety of environmental factors on the tidal flats, including sediment levels, nutrient concentrations, tidal heights, and salinity. Additionally, the ecological restoration project has the potential to artificially drive the succession of plant and animal communities in the NETF. These large-scale coastal projects have the capacity to artificially modify coastal habitats and promote biotic succession; therefore, further investigation into their potential effects on macroalgal distribution in the NETF is warranted.

4.3 The developmental history and ecological risks of *Ulva* in the NEFT

The invasion of green seaweed in intertidal salt marsh areas seems to have become a common phenomenon in recent years (Grimes et al., 2018; Nelson et al., 2021; Woodhouse and Zuccarello, 2023; Xia et al., 2023a, b). Similar to other relevant studies, the process of "establishment of micropropagules → establishment of *Ulva* populations → succession of *Ulva* species → localized outbreak of dominant species" by macroalgae in the intertidal zone is frequently overlooked. It is only when *Ulva* reaches a certain threshold of ecological risk (Lu et al., 2022; Hu et al., 2022) that it attracts significant attention from local residents, tourists, researchers, and governmental institutions.

Reflecting on the historical progression of green macroalgae occurrence and development in the NETF, we can delineate the following events: In March 2015, researchers cultivating intertidal vascular plants at the NETF observed a limited presence of green macroalgae in the intertidal zone. Subsequent identification revealed these attached green algae to be *Ulva flexuosa*, as described by Professor Peimin He from the College of Oceanography and Ecological Science at Shanghai Ocean University. In March 2019, during a study on *S. mariqueter* meadows coverage, researchers noted distinct changes in the morphology of attached green algae at the NETF and an expanded distribution range of these macroalgae. The green macroalgae attached to the detrital matrix of intertidal withered plants were discovered by Dr. Mingxuan Wu from the Royal Netherlands Institute for Sea Research (NIOZ). Upon identification, it was found that all the attached green algae present that year were *U. prolifera*, with no trace of *U. flexuosa*. It was not until 2021 that a localized outbreak of attached algal mats emerged in the intertidal zone of the NETF (Figures 2, 3). This outbreak featured *U. prolifera* (Figures 4-6), capturing our attention and concern. Sample collection was temporarily suspended from the second half of 2021 to the first half of 2024, as a result of beach closures and the impact of the COVID-19 pandemic. Nevertheless, this study provides background data before the green tide outbreak, which is often lacking in other sea areas where basic investigations are only carried out after such an event occurs. This offers a new perspective on the emergence and progression of green tide, as well as the critical considerations in implementing artificial construction projects in the intertidal zone.

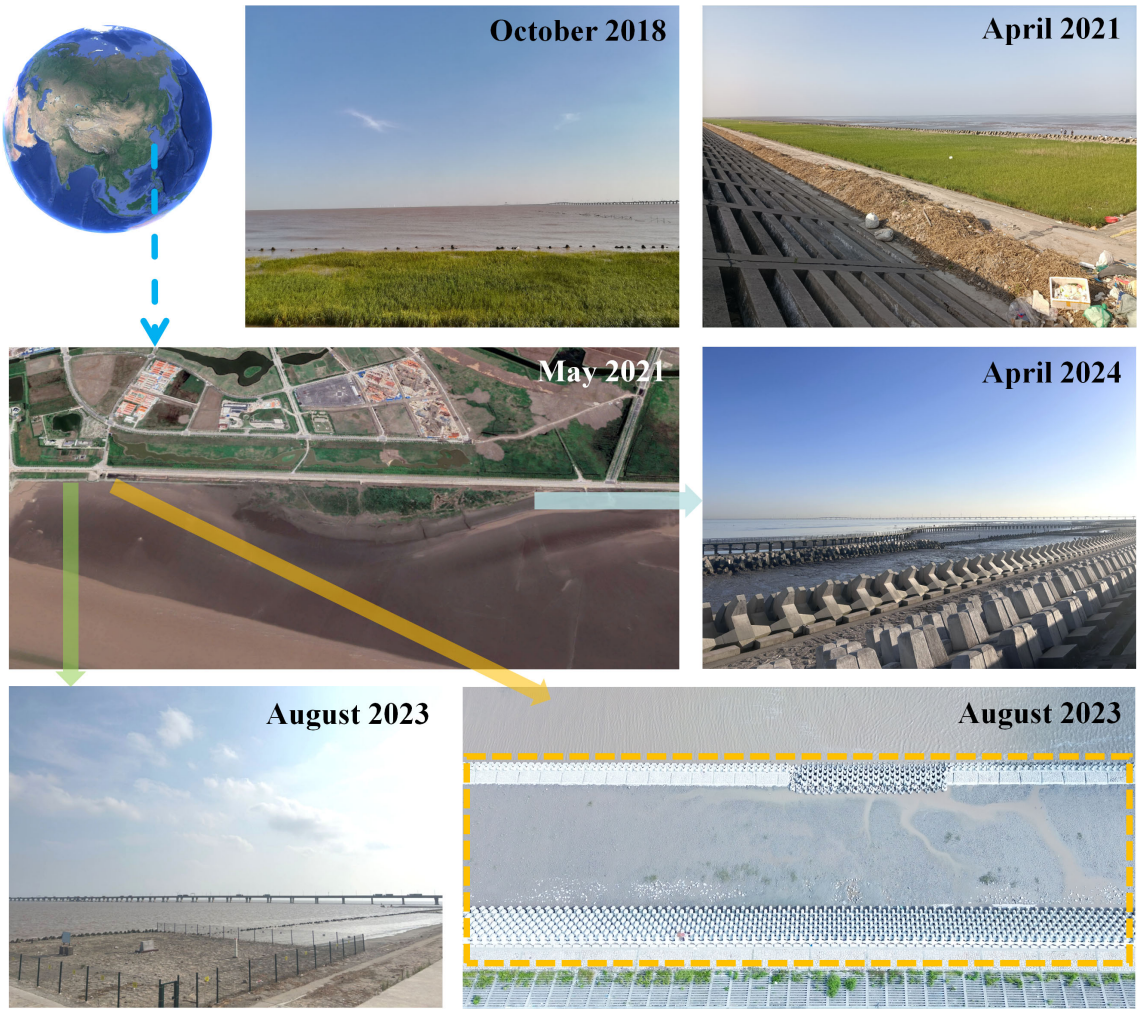

FIGURE 11
Schematic illustration of a section of the Nanhui-east-tidal-flat depicting the destruction of intertidal habitat before and after June 2021. Before June 2021, the yellow dashed area was rich in *Phragmites australis*, *Spartina alterniflora*, *Scirpus mariqueter*, and *Ulva prolifera* (also visible in Figure 2). Subsequent to the commencement of the Shanghai Lin-gang Coastal Ecological Protection and Restoration Project, the original intertidal vegetation in the yellow dashed area was significantly diminished, with only a small amount of *U. prolifera* remaining attached in certain regions.

Six potential sources of *Ulva* macroalgae or micropropagules in the intertidal zone of the NETF are proposed. Firstly, micropropagules may be released by attached *Ulva* macroalgae in the seaward channels of Shanghai. Secondly, from 2010 to 2013, researchers cultivated *Porphyra haitanensis* in the NETF (Huang et al., 2022). Meanwhile, filamentous thallus seedlings of *P. haitanensis* were cultivated in Xiangshan County, Ningbo City, Zhejiang Province. During the cultivation of filamentous thallus seedlings and net attachment stages of *Porphyra* cultivation, micropropagules of *Ulva* (Liu et al., 2013b) present in the local seawater of Xiangshan Bay often co-attached to the net curtains as harmful species. Subsequently, *Porphyra* net curtains were transported to the NETF for cultivation where *Ulva* micropropagules promptly developed into *Ulva* macroalgae. Thirdly, coastal areas of the Yellow Sea and East China Sea have long been impacted by large-scale green tide events (Hu et al., 2010; Xing and Hu, 2016; Min et al., 2019; Li et al., 2022; Cao et al., 2023; Luo et al., 2023; Qu et al., 2023; Xu et al., 2023; Feng et al., 2024). *Ulva* algae, which enters the East China Sea beyond the Yangtze River Estuary, releases micropropagules (Zhang et al., 2015). These micropropagules, along with *Ulva* macroalgae, may be transported into the NETF area by ocean currents and establish attachment. Fourthly, the natural distribution of *Ulva* macroalgae and micropropagules occurs in bays and islands of the East China Sea (Liu et al., 2013b; Tong et al., 2022), and these micropropagules may enter the NETF area via ocean currents. Fifthly, algae attached to floating marine debris and other carriers (Turner and Williams, 2021) may also enter the area and eventually establish attachment. Sixthly, Yangshan Port, the world's largest container port by throughput, is located approximately 15 nautical miles from the NETF. The vicinity of the NETF often witnesses the anchoring of ocean-going vessels, and the likelihood is high that ocean-going vessels' ballast water and sediments carry *Ulva* micropropagules (Flagella et al., 2007, 2010).

In any case, *Ulva* has already established attachment and formed localized algal mats in the NETF area. When *Ulva*

becomes the dominant species in the intertidal zone, it often indicates severe eutrophication and deteriorating ecological conditions in the local marine environment. The preliminary survey in 2024 found that algal mats were still present in the NETF (station F-H in this study). With the Shanghai Lin-gang Coastal Marine Ecological Conservation and Restoration Project nearing completion, following restoration and stabilization of the habitat in the NETF area, *Ulva* and its micropropagules will firmly attach, germinate, and continue to form extensive algal mats, and this phenomenon warrants attention from researchers. Research suggests that phenomena similar to large-scale harmful algal blooms in the Yellow Sea are unlikely to decrease in the short term and are expected to intensify in the future (Qi et al., 2022). As an "opportunistic" algal species (Xu et al., 2012; Zhao et al., 2018), the dominance of *Ulva* as a single species often signals the beginning of a localized and large-scale algal bloom outbreak. These blooms can exert profound adverse impacts on sandy or muddy intertidal habitats (Lyons et al., 2014), potentially influencing their biodiversity and ecosystem stability.

4.4 Current monitoring of green tide macroalgae in the NETF area primarily relies on field surveys

Concerns regarding the potential for a large-scale green tide in the NETF were not unfounded. These concerns materialized in mid-July 2023 when a small-scale green tide was detected near the East Sea Bridge (Figure 12). The emergency was confirmed by releasing a drone to patrol the area of floating macroalgae covering approximately 1 km^2 on July 13, 2023. However, the scale was relatively minor, with the floating macroalgae exhibiting a scattered distribution, and the algal coverage was low, being less than 0.01%. The biomass of these macroalgae, characterized by their small-scale and sporadic distribution, poses a challenge for conventional satellite remote sensing techniques to effectively monitor. Furthermore, this small-scale green tide did not continue to expand, and its impact on the local waters was relatively small, but it is worth raising the attention of researchers. The blooming macroalgae collected in the field (Figure 12) were identified morphologically and molecularly, and the only dominant species in the green tide was found to be *U. prolifera*. The researchers discovered the green tide outbreak approximately 5 nautical miles from NETF, situated in Hangzhou Bay, East China Sea. The sea area is under the jurisdiction of Shanghai Pudong New Area and is adjacent to the sea area of Shengsi County, Zhoushan City, Zhejiang Province. The available evidence is not sufficient to confirm that the small-scale floating *U. prolifera* in the Shanghai coastal area in mid-July 2023 was from the NETF, which will require a future long-period survey of green macroalgal distribution and shedding throughout Hangzhou Bay. It is hypothesized that it may be that the construction of the NETF Coastal Marine Ecological Conservation and Restoration Project in late June to early July 2023 resulted in releasing of attached *U. prolifera* and the formation of a small-scale green tide, or it may have been formed by natural shedding of sporadically distributed macroalgae in this area, which will require large-scale monitoring and traceability analyses for an extended period.

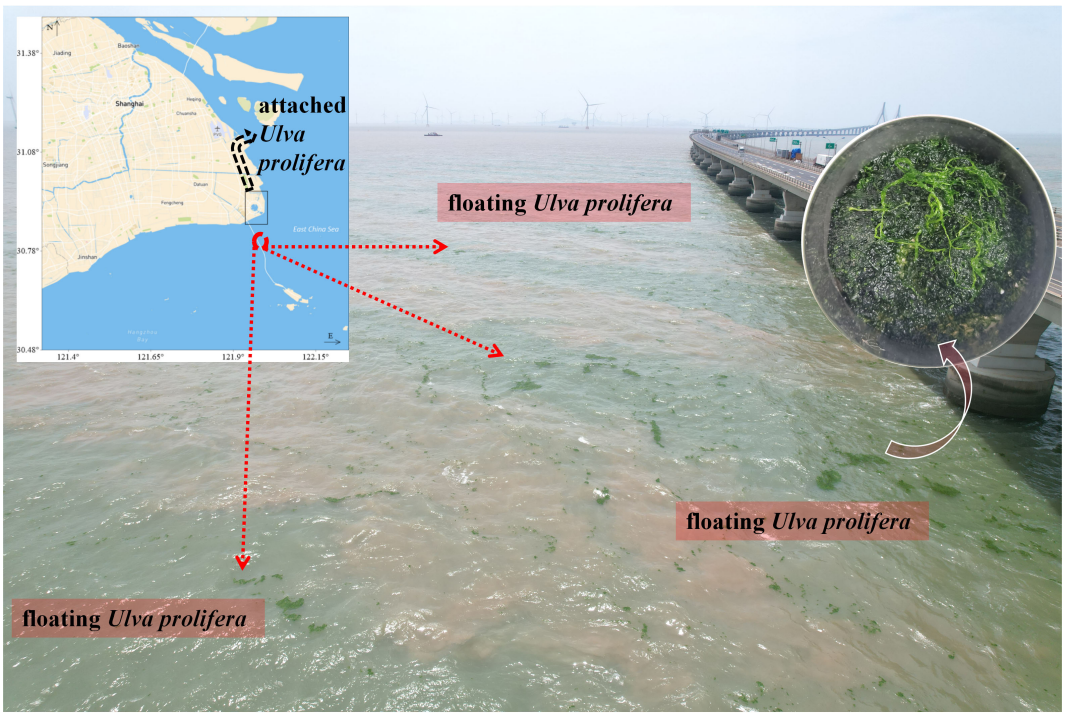

FIGURE 12
A small-scale green tide disaster occurred for the first time in the sea area near the Nanhui-east-tidal-flat in mid-July 2023.

Regarding the monitoring of algal distribution, the current mainstream methods include field surveys (on-site monitoring and drone patrol monitoring) and satellite remote sensing monitoring (Xia et al., 2024a). Among them, satellite remote sensing monitoring technology has a very broad application space during the outbreak of green tides (An et al., 2022; Zhang S. et al., 2022; Hu et al., 2023; Hu, 2024; Qi et al., 2023; Xing et al., 2023; Yu et al., 2023). The specific principle is based on the atmospherically corrected satellite surface reflectance signals, analyzing the spectral characteristics of green tide macroalgae and background water bodies, and using different remote sensing index algorithms (common remote sensing indices include Normalized Difference Vegetation Index, Phytoplankton Floating Algae Index, Difference Vegetation Index, Normalized Difference Algae Index, etc.) to carry out the identification of green tide macroalgae. However, it must be considered that satellite remote sensing monitoring technology is not always fully effective. On the one hand, the performance of different algorithms is easily affected by various observational conditions, including seawater background (turbid and clear seawater) and external observational conditions (such as cloud cover, solar flares, and observational geometry) (Hu et al., 2023). On the other hand, existing research and experience have found that satellite remote sensing monitoring technology is more suitable for monitoring large-scale harmful algal bloom phenomena, such as large-scale outbreaks of golden tides and green tides (Smetacek and Zingone, 2013; Xing and Hu, 2016; Wang et al., 2019; Liu et al., 2021b; Hu et al., 2023). Taking green tides as an example, the annual maximum coverage area of green tides in the Yellow Sea is tens to thousands of square kilometers (Sun et al., 2022a), and conventional satellite remote sensing monitoring technology typically can easily detect the presence of green tide macroalgae only in the middle and late stages of the outbreak (when the distribution area of algae is slightly larger and the coverage is higher); however, in the early and terminal stages of the outbreak, often due to the small distribution area of algae (or even though the distribution area is large, but the algae distribution is discontinuous) and low coverage, conventional satellite remote sensing monitoring technology often fails to detect the distribution of green tide macroalgae in a timely manner; this also leads to the fact that under current technological conditions, field surveys can effectively make up for the shortcomings of conventional satellite remote sensing monitoring technology (Song et al., 2022; Wang et al., 2023; Xia et al., 2024a), and can provide real-time information on algal species and the distribution status of algae, aiding in the early prevention and control of green tides (Sun et al., 2022a; Xia et al., 2024a).

Another case in point is the continuous outbreak of green tides in Qinhuangdao since 2015, which has also attracted the attention of researchers. Conventional satellite remote sensing monitoring technology also finds it difficult to detect green tide macroalgae in the floating stage in the Qinhuangdao Sea area; it is often only when a large amount of algal biomass is driven by wind and ocean currents and accumulates over a large area on the beach that visually striking algal mats (Xiao et al., 2021) are formed, with the scale of the floating green tide macroalgae being relatively limited before accumulating in the intertidal flats. Subsequent researchers mainly used field surveys and other methods to gradually determine that the main source of Qinhuangdao green tide macroalgae comes from the local sea area's subtidal seaweed fields (Han et al., 2019; Song et al., 2019a, b; Han et al., 2022a, b). The small-scale floating green tide macroalgae discovered by this study in mid-July 2023 is far smaller than the scale of the Yellow Sea green tide outbreak and the Qinhuangdao green tide outbreak; the Ministry of Natural Resources attempted to use conventional satellite data (such as MODIS series satellites, Landsat series satellites, Haiyang series satellites, etc.) to detect the small-scale green tide in the NETF sea area, but due to the small distribution area of algae, extremely low coverage, and the limited resolution of conventional satellite remote sensing monitoring technology, the small-scale green tide outbreak event was not successfully detected. Utilizing advanced ultra-high-resolution satellite remote sensing monitoring technology could potentially reveal extremely small-scale floating macroalgae. For instance, Zhang S. et al. (2022) successfully identified small-scale *Sargassum* mats accumulating on Miami Beach and Cancun Beach using 3-m resolution PlanetScope/Dove data. Nevertheless, this approach is limited by user access permissions, and the procurement cost of ultra-high-resolution satellite remote sensing imagery is often prohibitively expensive. When contemplating the initiation of regular monitoring and species diversity research at a low cost, field surveys constitute a significant approach for the early monitoring and warning of green tides.

At the same time, the conventional satellite remote sensing identification of intertidal attached green tide macroalgae has always been a challenge, and few studies have been able to successfully apply satellite remote sensing monitoring technology to identify small-scale attached algal mats in intertidal areas. Xing et al. (2023) applied satellite remote sensing and deep learning technology to identify large-scale attached green tide macroalgae in intertidal areas, and the successful conduct of this study benefited from three important conditions: first, Xing et al. (2023)' study area 2.07 km^2, the length, and width of the area are far greater than the resolution requirements of conventional satellite remote sensing monitoring technology; second, the area routinely experiences large-scale green tide outbreaks (the continuous coverage area of green tide algae is greater than 1 km^2), and there is an early research foundation on the main outbreak species and the preliminary distribution of algae; third, the intertidal area is dominated by the single dominant species *U. pertusa*, with no other higher plants, and only similar species distribution is conducive to satellite remote sensing monitoring. In this study, *U. prolifera* is distributed in the intertidal artificial habitat with a narrow strip feature (Figures 2B, C, 3B, 11), but the width of the habitat where *U. prolifera* is concentrated is about 28-31 meters; and within the area, green tide macroalgae and other higher plants are interwoven, with some higher plants are covered with *U. prolifera* (Figures 2B, 3C, D), the image resolution and species discrimination of existing conventional satellite remote sensing monitoring technology is difficult to effectively apply in this area. Unless advanced ultra-high-resolution satellite remote sensing monitoring technology is utilized (Zhang S. et al., 2022), it is unlikely to detect the small-scale algal mats present in the intertidal zone; considering the limited access to ultra-high-resolution satellite remote sensing imagery, the costly purchase of images, and the interference caused by the

numerous higher plants in the NETF area to the identification of algal distribution, the monitoring of green tide macroalgae in the NETF area currently relies on field surveys, as is the case with studies on other species in the NETF area (Wu et al., 2020, 2021; Wang MQ. et al., 2022; Gao et al., 2024; Li et al., 2024b; Zhao et al., 2024). Field surveys are a basic scientific research method based on on-site research (Song et al., 2019a, b; Liu et al., 2022; Li et al., 2023b; Xia et al., 2023b, c), which are suitable for the analysis of outbreak dominant species in the early stages of attached green tide macroalgae and biomass monitoring.

5 Conclusion

Based on morphological and molecular biological identification, researchers have confirmed that the green macroalgae along the coastline of the NETF from March 2021 to May were *U. prolifera*, characterized by wide blades, the ability to colonize a wide range of substrates in the intertidal zone, and obvious air bladders. The attached *U. prolifera* continued to grow, with the average biomass showing an increasing trend and reaching its peak on May 1st (within the accessible sampling period). Furthermore, environmental investigations suggested that high levels of eutrophication in the sea area as well as favorable environmental conditions contributed to the rapid proliferation of "opportunistic" *Ulva* in the NETF. Existing studies also demonstrate that the implementation of reclamation projects tends to exacerbate the outbreak of green tides (Kuang et al., 2024). In summary, anthropogenic disturbances, particularly continued reclamation activities, severely impact the NETF. It is crucial to maintain a balance between coastal resource development and marine ecological management given the high likelihood of future large-scale algal blooms in NETF; indeed, signs and preludes of a small-scale green tide were observed in July 2023, which requires further long-term monitoring and a set of disaster emergency management measures suitable for the local sea.

The difficulty in conducting large-scale monitoring lies in the substantial consumption of human, material, and financial resources, thus necessitating a case-by-case analysis. When studying attached green tide macroalgae and small-scale floating green tide macroalgae, field surveys are generally employed (Song et al., 2019a, b; Liu et al., 2022; Li et al., 2023b; Xia et al., 2023b, c); when the coverage area of attached green tide macroalgae is large and there are no higher plants or other growths in the habitat, satellite remote sensing monitoring technology can be attempted to confirm the distribution and coverage area of the attached green tide macroalgae (Xing et al., 2023); when tracing the origins or impact areas of large-scale floating green tide macroalgae, a combination of field surveys, micropropagules abundance studies, drift path numerical simulations, and satellite remote sensing monitoring are generally used (Huo et al., 2014; Zhang et al., 2015; Qi et al., 2016; Xing et al., 2019; Han et al., 2022a, b; Tong et al., 2022; Zhang S. et al., 2022; Hu et al., 2023; Xia et al., 2024b); when it comes to early warning and forecasting of large-scale green tide macroalgae floating paths, satellite remote sensing monitoring combined with field surveys is generally used (Sun et al., 2022a; Li et al., 2023c). This study focuses on the early distribution of attached green tide macroalgae in the NETF area, thus primarily conducting related research based on field survey methods; should the NETF area experience large-scale floating green tide macroalgae in the future (where the continuous coverage area of green tide macroalgae needs to be at least greater than 1 km^2), and if this leads to a significant marine ecological disaster, it would be very necessary to combine satellite remote sensing monitoring and other technologies to support the implementation of related early warning and prevention and control efforts.

Overall, the proliferation of extensive algal mats in the NETF area is a natural feedback mechanism in response to an imbalanced ecosystem. Similar to occurrences of *Ulva* outbreaks in other countries (Guidone and Thornber, 2013; Chavez-Sanchez et al., 2018), the growth and outbreak of *Ulva* demonstrate both periodicity and inevitability. The rapid expansion and outbreak of *Ulva* in China can be attributed to a favorable combination of factors, and it is not attributable to the species itself. The primary concern that needs to be addressed is the mitigation of nutrient enrichment in the marine environment (Liu et al., 2013a; Chavez-Sanchez et al., 2017; Lapointe et al., 2023). With China's rapid industrialization, future efforts to promote industrial modernization must be harmonized with ecological conservation. Effective management of pollution sources, including industrial, agricultural, and domestic wastewater discharge into rivers and seas, is essential, as well as initiatives for intensive phosphorus and nitrogen removal from sewage (Lapointe et al., 2023). Developed capitalist nations have dedicated decades to controlling algal blooms (He et al., 2019) and reducing nutrient enrichment in marine environments. Similarly, China faces a lengthy and challenging journey towards these objectives.

Data availability statement

The datasets presented in this study can be found in online repositories. The names of the repository/repositories and accession number(s) can be found in the article/supplementary material.

Author contributions

JL: Funding acquisition, Investigation, Project administration, Resources, Supervision, Writing – original draft, Writing – review & editing. ZX: Conceptualization, Resources, Writing – original draft. YZ: Conceptualization, Resources, Writing – original draft. JX: Conceptualization, Funding acquisition, Investigation, Methodology, Resources, Writing – original draft. PH: Funding acquisition, Project administration, Supervision, Writing – review & editing.

Funding

The author(s) declare financial support was received for the research, authorship, and/or publication of this article. This work was supported by the Youth Development Fund Project of the State

Key Laboratory of Marine Geology, the National Key Research & Development Program of China (2022YFC3106004; 2022YFC3106001), the Shanghai Super Postdoctoral Incentive Plan, and the Shanghai Ocean Bureau Project (Shanghai Ocean Science 2022-03).

Acknowledgments

Acknowledgment for the data support from the National Marine Data Center, National Science & Technology Resource Sharing Service Platform of China. Meanwhile, the author(s) would like to express their gratitude to the researchers at Xiamen University (Chongxiang Li), East China Normal University (Xiaoqian Yang), Shandong University (Yichao Tong), and Shanghai Ocean University (Shuang Zhao, Yuqing Sun and Yiyuan Tang) for their assistance in sample collection. Concurrently, Dr. Liu extends his sincere appreciation for the educational and formative contributions provided by Hebei University and Shanghai Ocean University. Furthermore, he expresses his gratitude for the assistance and support received from the Ministry of Natural Resources of the People's Republic of China.

Conflict of interest

The authors declare that the research was conducted in the absence of any commercial or financial relationships that could be construed as a potential conflict of interest.

Generative AI statement

The author(s) declare that no Generative AI was used in the creation of this manuscript.

Publisher's note

References

AbouGabal, A. A., Mohamed, A. A. E., Aboul-Ela, H. M., Khaled, A. A., Aly, H. M., Abdullah, M. I., et al. (2023). DNA barcoding of marine macroalgae as bioindicators of heavy metal pollution. *Mar. pollut. Bull.* 189, 114761. doi: 10.1016/j.marpolbul.2023.114761

Alsufyani, T., Califano, G., Deicke, M., Grueneberg, J., Weiss, A., Engelen, A. H., et al. (2020). Macroalgal bacterial interactions: identification and role of thallusin in morphogenesis of the seaweed *Ulva* (Chlorophyta). *J. Exp. Bot.* 71, 3340–3349. doi: 10.1093/jxb/eraa066

An, D. Y., Xing, Q. G., Yu, D. F., and Pan, S. Q. (2022). A simple method for estimating macroalgae area under clouds on MODIS imagery. *Front. Mar. Sci.* 9. doi: 10.3389/fmars.2022.995731

Barbier, E. B., Hacker, S. D., Kennedy, C., Koch, E. W., Stier, A. C., and Silliman, B. R. (2011). The value of estuarine and coastal ecosystem services. *Ecol. Monogr.* 81, 169–193. doi: 10.1890/10-1510.1

Blomster, J., Back, S., Fewer, D. P., Kiirikki, M., Lehvo, A., Maggs, C. A., et al. (2002). Novel morphology in *Enteromorpha* (Ulvophyceae) forming green tides. *Am. J. Bot.* 89, 1756–1763. doi: 10.3732/ajb.89.11.1756

Bodar, P. A., Iyer, S. L., and Mantri, V. A. (2024). Division pattern and evaluation of technical performance of bio-volume measurements of divided and un-divided cells in *Ulva ohnoi* for determining growth. *Thalassas* 40, 531–537. doi: 10.1007/s41208-023-00654-2

Cao, J. X., Liu, J. L., Zhao, S., Tong, Y. C., Li, S., Xia, Z. Y., et al. (2023). Advances in the research on micropropagules and their role in green tide outbreaks in the Southern Yellow Sea. *Mar. pollut. Bull.* 188, 114710. doi: 10.1016/j.marpolbul.2023.114710

Chavez-Sanchez, T., Pinon-Gimate, A., Serviere-Zaragoza, E., Lopez-Bautista, J. M., and Casas-Valdez, M. (2018). *Ulva* blooms in the southwestern Gulf of California: Reproduction and biomass. *Estuarine. Coast. Shelf. Sci.* 200, 202–211. doi: 10.1016/j.ecss.2017.11.007

Chavez-Sanchez, T., Pinon-Gimate, A., Serviere-Zaragoza, E., Sanchez-Gonzalez, A., Hernandez-Carmona, G., and Casas-Valdez, M. (2017). Recruitment in *Ulva* blooms in relation to temperature, salinity and nutrients in a subtropical bay of the Gulf of California. *Botanica Marina.* 60, 257–270. doi: 10.1515/bot-2016-0066

Chen, R. (2018). Preliminary study on epiphytic bacteria of *Ulva prolifera*. (Shanghai: Shanghai Ocean University), 1–39.

Chen, J. Q., Li, X. M., Wang, K., Zhang, S. Y., and Li, J. (2022). Estimation of seaweed biomass based on multispectral UAV in the intertidal zone of gouqi island. *Remote Sens.* 14, 2143. doi: 10.3390/rs14092143

Chi, W. Q., Shu, F. F., Lin, Y. T., Li, Y. H., Luo, F. S., He, J., et al. (2023). Typhoon-induced destruction and reconstruction of the coastal current system on the inner shelf of East China Sea. *Continental. Shelf. Res.* 255, 104912. doi: 10.1016/j.csr.2022.104912

Choi, T. S., and Kim, K. Y. (2004). Spatial pattern of intertidal macroalgal assemblages associated with tidal levels. *Hydrobiologia* 512, 49–56. doi: 10.1023/B:HYDR.0000020309.72972.17

Crain, C. M., Halpern, B. S., Beck, M. W., and Kappel, C. V. (2009). Understanding and managing human threats to the coastal marine environment. *Year. Ecol. Conserv. Biol.* 1162, 39–62. doi: 10.1111/j.1749-6632.2009.04496.x

Cui, J. J., Zhang, J. H., Huo, Y. Z., Zhou, L. J., Wu, Q., Chen, L. P., et al. (2015). Adaptability of free-floating green tide algae in the Yellow Sea to variable temperature and light intensity. *Mar. pollut. Bull.* 101, 660–666. doi: 10.1016/j.marpolbul.2015.10.033

Dartois, M., Pante, E., Viricel, A., Becquet, V., and Sauriau, P. G. (2021). Molecular genetic diversity of seaweeds morphologically related to *Ulva rigida* at three sites along the French Atlantic coast. *PeerJ* 9, e11966. doi: 10.7717/peerj.11966

de Guimaraens, M. A., and Coutinho, R. (2000). Temporal and spatial variation of *Ulva* spp. and water properties in the Cabo Frio upwelling region of Brazil. *Aquat. Bot.* 66, 101–114. doi: 10.1016/S0304-3770(99)00070-4

Du, G. Y., Wu, F. F., Mao, Y. X., Guo, S. H., Xue, H. F., and Bi, G. Q. (2014). DNA barcoding assessment of green macroalgae in coastal zone around Qingdao, China. *J. Ocean. Univ. China* 13, 97–103. doi: 10.1007/s11802-014-2197-1

Duan, W. J., Guo, L., Sun, D., Zhu, S. F., Chen, X. F., Zhu, W. R., et al. (2012). Morphological and molecular characterization of free-floating and attached green macroalgae *Ulva* spp. in the Yellow Sea of China. *J. Appl. Phycol.* 24, 97–108. doi: 10.1007/s10811-011-9654-7

Duarte, C. M., Losada, I. J., Hendriks, I. E., Mazarrasa, I., and Marba, N. (2013). The role of coastal plant communities for climate change mitigation and adaptation. *Nat. Climate Change* 3, 961–968. doi: 10.1038/NCLIMATE1970

Fan, D. D., Guo, Y. X., Wang, P., and Shi, J. Z. (2006). Cross-shore variations in morphodynamic processes of an open-coast mudflat in the Changjiang Delta, China: With an emphasis on storm impacts. *Continental. Shelf. Res.* 26, 517–538. doi: 10.1016/j.csr.2005.12.011

Farasat, M., Khavari-Nejad, R. A., Nabavi, S. M. B., and Namjooyan, F. (2014). Antioxidant activity, total phenolics and flavonoid contents of some edible green seaweeds from northern coasts of the persian gulf. *Iranian. J. Pharm. Res.* 13, 163–170.

Feng, Y., Xiong, Y. L., Hall-Spencer, J. M., Liu, K. L., Beardall, J., Gao, K. S., et al. (2024). Shift in algal blooms from micro- to macroalgae around China with increasing eutrophication and climate change. *Global Change Biol.* 30, e17018. doi: 10.1111/gcb.17018

Flagella, M. M., Andreakis, N., Hiraoka, M., Verlaque, M., and Buia, M. C. (2010). Identification of cryptic *Ulva* species (Chlorophyta, Ulvales) transported by ballast water. *J. Biol. Research-Thessaloniki.* 13, 47–57.

Flagella, M. M., Verlaque, M., Soria, A., and Buia, M. C. (2007). Macroalgal survival in ballast water tanks. *Mar. pollut. Bull.* 54, 1395–1401. doi: 10.1016/j.marpolbul.2007.05.015

Fort, A., Mannion, C., Farinas-Franco, J. M., and Sulpice, R. (2020). Green tides select for fast expanding *Ulva* strains. *Sci. Total. Environ.* 698, 134337. doi: 10.1016/j.scitotenv.2019.134337

Gao, X. F., He, N., Fang, S. B., Zhang, B. L., Wang, M. Q., and He, P. M. (2024). The above and the belowground nitrogen allocation strategy of *Scirpus mariqueter* based on ^{15}N isotope tracing along an elevation gradient and its significance for coastal wetlands restoration. *J. Plant Nutr. Soil Sci.* 187, 504–515. doi: 10.1002/jpln.202400070

Gao, G., Zhong, Z. H., Zhou, X. H., and Xu, J. T. (2016). Changes in morphological plasticity of *Ulva prolifera* under different environmental conditions: A laboratory experiment. *Harmful. Algae.* 59, 51–58. doi: 10.1016/j.hal.2016.09.004

Ge, Z. M., Tian-Hou, W. B., Zhou, X., Wang, K. Y., and Shi, W. Y. (2007). Changes in the spatial distribution of migratory shorebirds along the Shanghai shoreline, China, between 1984 and 2004. *Emu-Austral. Ornithol.* 107, 19–27. doi: 10.1071/MU05048

Graba-Landry, A., Hoey, A. S., Matley, J. K., Sheppard-Brennand, H., Poore, A. G. B., Byrne, M., et al. (2018). Ocean warming has greater and more consistent negative effects than ocean acidification on the growth and health of subtropical macroalgae. *Mar. Ecol. Prog. Ser.* 595, 55–69. doi: 10.3354/meps12552

Grimes, S., Benabdi, M., Babali, N., Refes, W., Boudjellal-Kaidi, N., and Seridi, H. (2018). Biodiversity changes along the Algerian coast (Southwestern Mediterranean basin) from 1834 to 2017. First assessment of introduced species. *Mediterr. Mar. Sci.* 19, 156–179. doi: 10.12681/mms.13824

Guidone, M., and Thornber, C. S. (2013). Examination of *Ulva* bloom species richness and relative abundance reveals two cryptically co-occurring bloom species in Narragansett Bay, Rhode Island. *Harmful. Algae.* 24, 1–9. doi: 10.1016/j.hal.2012.12.007

Han, H. B., Li, Y., Ma, X. J., Song, W., Wang, Z. L., and Zhang, X. L. (2022a). Factors influencing the spatial and temporal distributions of green algae micro-propagules in the coastal waters of Jinmenghaiwan, Qinhuangdao, China. *Mar. pollut. Bull.* 175, 113328. doi: 10.1016/j.marpolbul.2022.113328

Han, H. B., Li, Y., Wang, Z. L., Song, W., and Ma, X. J. (2022b). Tempo-spatial distribution and species composition of green algae micro-propagules in the coastal waters of Qinhuangdao after green tides bloom in 2020. *Estuarine. Coast. Shelf. Sci.* 276, 108054. doi: 10.1016/j.ecss.2022.108054

Han, Z., Liu, Y., Guo, Y. F., Zhang, H., and Yun, C. X. (2010). "Spatial and temporal variations of vegetation communities in the Shanghai Nanhui tidal flat over 60 years," in *6th International Symposium on Digital Earth–Data Processing and Applications*, (Chinese Nat. Comm. Int. Soc. Digital Earth/Ctr. Earth Observ. Digital Earth, Chi, Beijing, P.R. China: Proc. SPIE), 7841, 784119. doi: 10.1117/12.873255

Han, H. B., Song, W., Wang, Z. L., Ding, D. W., Yuan, C., Zhang, X. L., et al. (2019). Distribution of green algae micro-propagules and their function in the formation of the green tides in the coast of Qinhuangdao, the Bohai Sea, China. *Acta Oceanol. Sin.* 38, 72–77. doi: 10.1007/s13131-018-1278-1

Hayden, H. S., Blomster, J., Maggs, C. A., Silva, P. C., Stanhope, M. J., and Waaland, J. R. (2003). Linnaeus was right all along: *Ulva* and *Enteromorpha* are not distinct genera. *Eur. J. Phycol.* 38, 277–294. doi: 10.1080/1364253031000136321

He, R. Y., Zeng, Y. Q., Zhao, S., Zhang, J. H., He, P. M., and Liu, J. L. (2023). Use of citric acid-activated chlorine dioxide to control *Ulva prolifera*. *Mar. pollut. Bull.* 194, 115357. doi: 10.1016/j.marpolbul.2023.115357

He, P. M., Zhang, J. H., Huo, Y. Z., and Cai, C. E. (2019). *Green tides of China* (Beijing: Science Press), 1–438.

Hu, C. M. (2024). A depth-invariant index to map floating algae: a conceptual design. *Remote Sens. Lett.* 15, 1–9. doi: 10.1080/2150704X.2023.2294746

Hu, C. M., Li, D. Q., Chen, C. S., Ge, J. Z., Muller-Karger, F. E., Liu, J. P., et al. (2010). On the recurrent *Ulva prolifera* blooms in the Yellow Sea and East China Sea. *J. Geophys. Research-Oceans.* 115, C05017. doi: 10.1029/2009jc005561

Hu, C. M., Qi, L., Hu, L. B., Cui, T. W., Xing, Q. G., He, M. X., et al. (2023). Mapping *Ulva prolifera* green tides from space: A revisit on algorithm design and data products. *Int. J. Appl. Earth Observ. Geoinformation.* 116, 103173. doi: 10.1016/j.jag.2022.103173

Hu, M. J., Zhao, S., Liu, J. L., Tong, Y. C., Xia, Z. Y., Xia, J., et al. (2022). The morphology, genetic diversity, and distribution of *Ulva meridionalis* (Ulvaceae, chlorophyta) in chinese seas. *J. Mar. Sci. Eng.* 10, 1873. doi: 10.3390/jmse10121873

Huang, L. B., Chen, J. H., and Yan, X. H. (2022). Cultivation experiment of *Porphyra haitanensis* in low-salinity sea area of Shanghai. *Fisheries. Sci. Technol. Inf.* 49, 15–18. doi: 10.16446/j.fsti.20210200117

Human, L. R. D., Adams, J. B., and Allanson, B. R. (2016). Insights into the cause of an *Ulva lactuca* Linnaeus bloom in the Knysna Estuary. *South Afr. J. Bot.* 107, 55–62. doi: 10.1016/j.sajb.2016.05.016

Huo, Y. Z., Hua, L., Wu, H. L., Zhang, J. H., Cui, J. J., Huang, X. W., et al. (2014). Abundance and distribution of *Ulva* microscopic propagules associated with a green tide in the southern coast of the Yellow Sea. *Harmful. Algae.* 39, 357–364. doi: 10.1016/j.hal.2014.09.008

Ichihara, K., Miyaji, K., and Shimada, S. (2013). Comparing the low-salinity tolerance of *Ulva* species distributed in different environments. *Phycol. Res.* 61, 52–57. doi: 10.1111/j.1440-1835.2012.00668.x

Innes, D. J. (1988). Genetic differentiation in the intertidal zone in populations of the alga *Enteromorpha linza* (Ulvales: Chlorophyta). *Mar. Biol.* 97, 9–16. doi: 10.1007/BF00391240

Kennish, M. J. (2002). Environmental threats and environmental future of estuaries. *Environ. Conserv.* 29, 78–107. doi: 10.1017/S0376892902000061

Kimura, M. (1980). A simple method for estimating evolutionary rates of base substitutions through comparative studies of nucleotide sequences. *J. Mol. Evol.* 16, 111–120. doi: 10.1007/BF01731581

Krause-Jensen, D., and Duarte, C. M. (2016). Substantial role of macroalgae in marine carbon sequestration. *Nat. Geosci.* 9, 737–742. doi: 10.1038/NGEO2790

Kuang, C. P., Wang, D., Wang, G., Liu, J. T., Han, X. J., and Li, Y. (2024). Impact of reclamation projects on water quality in Jinmeng bay, China. *Estuarine. Coast. Shelf. Sci.* 300, 108719. doi: 10.1016/j.ecss.2024.108719

Kumar, S., Stecher, G., Li, M., Knyaz, C., and Tamura, K. (2018). Molecular evolutionary genetics analysis across computing platforms. *Mol. Biol. Evol.* 35, 1547–1549. doi: 10.1093/molbev/msy096

Lapointe, B. E., Brewton, R. A., Wilking, L. E., and Herren, L. W. (2023). Fertilizer restrictions are not sufficient to mitigate nutrient pollution and harmful algal blooms in the Indian River Lagoon, Florida. *Mar. pollut. Bull.* 193, 115041. doi: 10.1016/j.marpolbul.2023.115041

Letunic, I., and Bork, P. (2021). Interactive Tree Of Life (iTOL) v5: an online tool for phylogenetic tree display and annotation. *Nucleic Acids Res.* 49, W293–W296. doi: 10.1093/nar/gkab301

Levin, L. A., Boesch, D. F., Covich, A., Dahm, C., Erseus, C., Ewel, K. C., et al. (2001). The function of marine critical transition zones and the importance of sediment biodiversity. *Ecosystems* 4, 430–451. doi: 10.1007/s10021-001-0021-4

Li, Y. H., Jiang, J. N., Zhang, R. H., Qie, W. D., Shao, J. Z., Zhu, W. R., et al. (2024a). Effects of photoperiod on the growth and physiological responses in *Ulva prolifera* under constant and diurnal temperature difference conditions. *Mar. Environ. Res.* 197, 106477. doi: 10.1016/j.marenvres.2024.106477

Li, Y., Ma, X. J., Jiang, M. J., Song, W., and Han, H. B. (2023b). Annual patterns of green tides blooms in the coastal waters of Qinhunagdao from 2018 to 2020. *J. Sea. Res.* 196, 102461. doi: 10.1016/j.seares.2023.102461

Li, Q., Ma, C. A., Lv, W. W., Tian, W., Yv, J., and Zhao, Y. L. (2012). Variations of 'zooplankton's community structure in reclaimed waters of Nanhui east tidal flat of Shanghai, East China. *Chin. J. Appl. Ecol.* 23, 2287–2294. doi: 10.13287/j.1001-9332.2012.0319

Li, C. X., Tang, Y. Y., Sun, W. H., Xia, J., Xia, Z. Y., Zhang, J. H., et al. (2023a). Physiological responses of *Ampithoe valida* and its feeding potential on *Ulva prolifera*. *Mar. Environ. Res.* 186, 105942. doi: 10.1016/j.marenvres.2023.105942

Li, Y. H., Wang, D., Xu, X. T., Gao, X. X., Sun, X., and Xu, N. J. (2017). Physiological responses of a green algae (*Ulva prolifera*) exposed to simulated acid rain and decreased salinity. *Photosynthetica* 55, 623–629. doi: 10.1007/s11099-017-0689-0

Li, S. Q., Xu, Z. H., and Wang, C. W. (2022). Public's preference for the treatment of *Ulva prolifera* blooms: A choice experiment study in China. *Algal. Research-Biomass. Biofuels Bioproducts.* 66, 102776. doi: 10.1016/j.algal.2022.102776

Li, T. Y., Xue, L. M., Zhang, X. M., Ma, Y. X., Gong, L., Shi, B. W., et al. (2024b). Harvested *Spartina* area performs better than native *Scirpus* in sedimentation and carbon preservation under storm surge. *Ocean. Coast. Manage.* 249, 107002. doi: 10.1016/j.ocecoaman.2023.107002

Li, C., Zhu, X. Y., Li, X. W., Jiang, S., Shi, H., Zhang, Y., et al. (2023c). All-weather monitoring of *Ulva prolifera* in the yellow sea based on sentinel-1, sentinel-3, and NPP satellite data. *Remote Sens.* 15, 5772. doi: 10.3390/rs15245772

Lin, A. P., Wang, C., Pan, G. H., Song, L. Y., Gao, S., Xie, X. J., et al. (2011). Diluted seawater promoted the green tide of *Ulva prolifera* (Chlorophyta, Ulvales). *Phycol. Res.* 59, 295–304. doi: 10.1111/j.1440-1835.2011.00629.x

Liu, W., Bao, Y. L., Li, K. J., Yang, N., He, P. M., He, C. Q., et al. (2024b). The diversity of planktonic bacteria driven by environmental factors in different mariculture areas in the East China Sea. *Mar. pollut. Bull.* 201, 116136. doi: 10.1016/j.marpolbul.2024.116136

Liu, F., Pang, S. J., Chopin, T., Gao, S. Q., Shan, T. F., Zhao, X. B., et al. (2013a). Understanding the recurrent large-scale green tide in the Yellow Sea: Temporal and spatial correlations between multiple geographical, aquacultural and biological factors. *Mar. Environ. Res.* 83, 38–47. doi: 10.1016/j.marenvres.2012.10.007

Liu, F., Pang, S. J., and Zhao, X. B. (2013b). Molecular phylogenetic analyses of *Ulva* (Chlorophyta, Ulvophyceae) mats in the Xiangshan Bay of China using high-resolution DNA markers. *J. Appl. Phycol.* 25, 1287–1295. doi: 10.1007/s10811-012-9955-5

Liu, J. L., Tong, Y. C., Xia, J., Sun, Y. Q., Zhao, X. H., Sun, J. Y., et al. (2022). *Ulva* macroalgae within local aquaculture ponds along the estuary of Dagu River, Jiaozhou Bay, Qingdao. *Mar. pollut. Bull.* 174, 113243. doi: 10.1016/j.marpolbul.2021.113243

Liu, J. L., Xia, J., Zhuang, M. M., Zhang, J. H., Sun, Y. Q., Tong, Y. C., et al. (2021b). Golden seaweed tides accumulated in *Pyropia* aquaculture areas are becoming a normal phenomenon in the Yellow Sea of China. *Sci. Total. Environ.* 774, 145726. doi: 10.1016/j.scitotenv.2021.145726

Liu, J. L., Xia, J., Zhuang, M. M., Zhang, J. H., Yu, K. F., Zhao, S., et al. (2021a). Controlling the source of green tides in the Yellow Sea: NaClO treatment of *Ulva* attached on *Pyropia* aquaculture rafts. *Aquaculture* 535, 736378. doi: 10.1016/j.aquaculture.2021.736378

Liu, J. L., Yuan, H. Q., Xia, Z. Y., and He, P. M. (2024a). Paying attention to the safety of global edible seaweeds after the discharge of nuclear-contaminated water from Japan.

Algal. Research-Biomass. Biofuels Bioproducts. 84, 103811. doi: 10.1016/j.algal.2024.103811

Loughnane, C. J., McIvor, L. M., Rindi, F., Stengel, D. B., and Guiry, M. D. (2008). Morphology, *rbc*L phylogeny and distribution of distromatic *Ulva* (Ulvophyceae, Chlorophyta) in Ireland and southern Britain. *Phycologia* 47, 416–429. doi: 10.2216/PH07-61.1

Lu, X. Q., Xu, H., Zhao, S., Kong, F. Z., Yan, T., and Jiang, P. (2022). The green tide in Yingkou, China in summer 2021 was caused by a subtropical alga-*Ulva meridionalis* (Ulvophyceae, Chlorophyta). *J. Oceanol. Limnol.* 40, 2354–2363. doi: 10.1007/s00343-022-2014-4

Luo, H. T., Yang, Y. F., and Xie, S. G. (2023). The ecological effect of large-scale coastal natural and cultivated seaweed litter decay processes: An overview and perspective. *J. Environ. Manage.* 341, 118091. doi: 10.1016/j.jenvman.2023.118091

Lyons, D. A., Arvanitidis, C., Blight, A. J., Chatzinikolaou, E., Guy-Haim, T., Kotta, J., et al. (2014). Macroalgal blooms alter community structure and primary productivity in marine ecosystems. *Global Change Biol.* 20, 2712–2724. doi: 10.1111/gcb.12644

Ma, C. A. (2015). *Influence of reclamation projects on the macrobenthos of Nanhui and Chongming east tidal flats* (Shanghai: East China Normal University), 1–133.

Ma, Y. Y., Zhao, J., Xie, W. F., and Jiang, P. (2020). Branching phenotype and plasticity in floating ecotype of *Ulva prolifera* (Ulvophyceae, Chlorophyta). *Mar. Sci.* 44, 98–105. doi: 10.11759/hykx20200121001

Mcleod, E., Chmura, G. L., Bouillon, S., Salm, R., Bjork, M., Duarte, C. M., et al. (2011). A blueprint for blue carbon: toward an improved understanding of the role of vegetated coastal habitats in sequestering CO_2. *Front. Ecol. Environ.* 9, 552–560. doi: 10.1890/110004

Mei, X. F., Dai, Z. J., Wei, W., Li, W. H., Wang, J., and Sheng, H. (2018). Secular bathymetric variations of the North Channel in the Changjiang (Yangtze) Estuary, China 1880-2013: causes and effects. *Geomorphology* 303, 30–40. doi: 10.1016/j.geomorph.2017.11.014

Min, S. H., Hwang, J. D., Oh, H. J., and Son, Y. B. (2019). Reflectivity characteristics of the green and golden tides from the Yellow Sea and East China Sea. *J. Coast. Res.* 90, 310–316. doi: 10.2112/si90-039.1

Nelson, W. A., D'Archino, R., Neill, K. F., and Robinson, N. M. (2021). Introduced marine macroalgae: new perspectives on species recognition and distribution in New Zealand. *Botanica Marina.* 64, 379–393. doi: 10.1515/bot-2021-0042

Niu, J. Y., Zou, Y. A., Yuan, X., Zhang, B., and Wang, T. H. (2013). Waterbird distribution patterns and environmentally impacted factors in reclaimed coastal wetlands of the eastern end of Nanhui county, Shanghai, China. *Acta Zool. Acad. Sci. Hungaricae.* 59, 171–185.

Park, C. S., and Hwang, E. K. (2011). An investigation of the relationship between sediment particles size and the development of green algal mats (*Ulva prolifera*) on the intertidal flats of Muan, Korea. *J. Appl. Phycol.* 23, 515–522. doi: 10.1007/s10811-010-9620-9

Peter, N. R., Raja, N. R., Rengarajan, J., Pillai, A. R., Kondusamy, A., Saravanan, A. K., et al. (2024). A comprehensive study on ecological insights of *Ulva lactuca* seaweed bloom in a lagoon along the southeast coast of India. *Ocean. Coast. Manage.* 248, 106964. doi: 10.1016/j.ocecoaman.2023.106964

Qi, L., Hu, C. M., Barnes, B. B., Lapointe, B. E., Chen, Y. L., Xie, Y. Y., et al. (2022). Climate and anthropogenic controls of seaweed expansions in the east China sea and yellow sea. *Geophys. Res. Lett.* 49, e2022GL098185. doi: 10.1029/2022GL098185

Qi, L., Hu, C. M., Xing, Q. G., and Shang, S. L. (2016). Long-term trend of *Ulva prolifera* blooms in the western Yellow Sea. *Harmful. Algae.* 58, 35–44. doi: 10.1016/j.hal.2016.07.004

Qi, L., Wang, M. H., and Hu, C. M. (2023). Uncertainties in MODIS-derived *Ulva prolifera* amounts in the yellow sea: A systematic evaluation using sentinel-2/MSI observations. *IEEE Geosci. Remote Sens. Lett.* 20, 1501805. doi: 10.1109/LGRS.2023.3272889

Qu, T. F., Zhao, X. Y., Guan, C., Hou, C. Z., Chen, J., Zhong, Y., et al. (2023). Structure-function covariation of phycospheric microorganisms associated with the typical cross-regional harmful macroalgal bloom. *Appl. Environ. Microbiol.* 89, e01815–e01822. doi: 10.1128/aem.01815-22

Raposo, M. F. D., de Morais, A. M. B., and de Morais, R. M. S. C. (2015). Marine polysaccharides from algae with potential biomedical applications. *Mar. Drugs* 13, 2967–3028. doi: 10.3390/md13052967

Riera, P., Stal, L., and Nieuwenhuize, J. (2004). Utilization of food sources by invertebrates in a man-made intertidal ecosystem (Westerschelde, the Netherlands): a $\delta^{13}C$ and $\delta^{15}N$ study. *J. Mar. Biol. Assoc. United. Kingdom.* 84, 323–326. doi: 10.1017/S0025315404009210h

Rybak, A. S. (2018). Species of *Ulva* (Ulvophyceae, Chlorophyta) as indicators of salinity. *Ecol. Indic.* 85, 253–261. doi: 10.1016/j.ecolind.2017.10.061

Rybak, A. S. (2021). Freshwater macroalga, *Ulva pilifera* (Ulvaceae, Chlorophyta) as an indicator of the trophic state of waters for small water bodies. *Ecol. Indic.* 121, 106951. doi: 10.1016/j.ecolind.2020.106951

Sasaki, Y. N., and Umeda, C. (2021). Rapid Warming of Sea Surface Temperature along the Kuroshio and the China Coast in the East China Sea during the Twentieth Century. *J. Climate* 34, 4803–4815. doi: 10.1175/JCLI-D-20-0421.1

Shimada, S., Yokoyama, N., Arai, S., and Hiraoka, M. (2008). Phylogeography of the genus *Ulva* (Ulvophyceae, Chlorophyta), with special reference to the Japanese freshwater and brackish taxa. *J. Appl. Phycol.* 20, 979–989. doi: 10.1007/s10811-007-9296-y

Smetacek, V., and Zingone, A. (2013). Green and golden seaweed tides on the rise. *Nature* 504, 84–88. doi: 10.1038/nature12860

Song, W., Han, H. B., Wang, Z. L., and Li, Y. (2019a). Molecular identification of the macroalgae that cause green tides in the Bohai Sea, China. *Aquat. Bot.* 156, 38–46. doi: 10.1016/j.aquabot.2019.04.004

Song, M. J., Kong, F. Z., Li, Y. F., Zhao, J., Yu, R. C., Zhou, M. J., et al. (2022). A massive green tide in the yellow sea in 2021: field investigation and analysis. *Int. J. Environ. Res. Public Health* 19, 11753. doi: 10.3390/ijerph191811753

Song, W., Wang, Z. L., Li, Y., Han, H. B., and Zhang, X. L. (2019b). Tracking the original source of the green tides in the Bohai Sea, China. *Estuarine. Coast. Shelf. Sci.* 219, 354–362. doi: 10.1016/j.ecss.2019.02.036

Sun, Y. Q., Liu, J. L., Xia, J., Tong, Y. C., Li, C. X., Zhao, S., et al. (2022b). Research development on resource utilization of green tide algae from the Southern Yellow Sea. *Energy Rep.* 8, 295–303. doi: 10.1016/j.egyr.2022.01.168

Sun, C. C., Wu, W. T., Liu, J., and Zang, J. Y. (2023). Contribution of freshwater aquaculture for nitrogen and phosphorus production in the Changjiang River and its impact on estuarine environment. *Prog. Fishery. Sci.* 44, 35–46. doi: 10.19663/j.issn2095-9869.20210820003

Sun, Y. Q., Yao, L. L., Liu, J. L., Tong, Y. C., Xia, J., Zhao, X. H., et al. (2022a). Prevention strategies for green tides at source in the Southern Yellow Sea. *Mar. pollut. Bull.* 178, 113646. doi: 10.1016/j.marpolbul.2022.113646

Tang, Y. L., Huangfu, J. L., Huang, R. H., and Chen, W. (2020). Surface warming reacceleration in offshore China and its interdecadal effects on the East Asia-Pacific climate. *Sci. Rep.* 10, 14811. doi: 10.1038/s41598-020-71862-6

Tao, Y. D., Yv, K. F., He, P. M., Sun, B., Li, C. W., Zhao, M., et al. (2017). Distribution of *Scirpus mariqueter* on nanhui coasts after reclamation and the associated affecting factors. *Resour. Environ. Yangtze. Basin.* 26, 1032–1041. doi: 10.11870/cjlyzyyhj201707009

Tian, B., Wu, W. T., Yang, Z. Q., and Zhou, Y. X. (2016). Drivers, trends, and potential impacts of long-term coastal reclamation in China from 1985 to 2010. *Estuarine. Coast. Shelf. Sci.* 170, 83–90. doi: 10.1016/j.ecss.2016.01.006

Tong, Y. C., Tang, P. C., Sun, Y. Q., Zhao, S., Zhang, J. H., Liu, J. L., et al. (2022). Distribution characteristics of green algal micro-propagules in the East China Sea in winter and their relationship with green tide macroalgae in the Yellow Sea. *J. Sea. Res.* 190, 102308. doi: 10.1016/j.seares.2022.102308

Turner, A., and Williams, T. (2021). The role of kelp in the transport and fate of negatively buoyant marine plastic. *J. Sea. Res.* 175, 102087. doi: 10.1016/j.seares.2021.102087

Wang, M. Q., Hu, C. M., Barnes, B. B., Mitchum, G., Lapointe, B., and Montoya, J. P. (2019). The great Atlantic *Sargassum* belt. *Science* 365, 83–87. doi: 10.1126/science.aaw7912

Wang, M. Q., Hu, Y., He, N., Wu, M. X., Wu, P. L., Wang, Q. Y., et al. (2022). The spatio-temporal patterns of macro benthos functional groups and the associated factors affecting them after wetland restoration. *J. Resour. Ecol.* 13, 1152–1164. doi: 10.5814/j.issn.1674-764x.2022.06.019

Wang, J. Y., Mo, D. X., Hou, Y. J., Li, S. Q., Li, J., Du, M., et al. (2022). The impact of typhoon intensity on wave height and storm surge in the northern east China sea: A comparative case study of typhoon muifa and typhoon lekima. *J. Mar. Sci. Eng.* 10, 192. doi: 10.3390/jmse10020192

Wang, Z. L., Xiao, J., Yuan, C., Miao, X. X., Fan, S. L., Fu, M. Z., et al. (2023). The drifting and spreading mechanism of floating *Ulva* mass in the waterways of Subei shoal, the Yellow Sea of China – Application for abating the world's largest green tides. *Mar. pollut. Bull.* 190, 114789. doi: 10.1016/j.marpolbul.2023.114789

Wei, W., Dai, Z. J., Mei, X. F., Liu, J. P., Gao, S., and Li, S. S. (2017). Shoal morphodynamics of the Changjiang (Yangtze) estuary: Influences from river damming, estuarine hydraulic engineering and reclamation projects. *Mar. Geol.* 386, 32–43. doi: 10.1016/j.margeo.2017.02.013

Wei, W., Tang, Z. H., Dai, Z. J., Lin, Y. F., Ge, Z. P., and Gao, J. J. (2015). Variations in tidal flats of the Changjiang (Yangtze) estuary during 1950s-2010s: Future crisis and policy implication. *Ocean. Coast. Manage.* 108, 89–96. doi: 10.1016/j.ocecoaman.2014.05.018

Wichard, T. (2015). Exploring bacteria-induced growth and morphogenesis in the green macroalga order Ulvales (Chlorophyta). *Front. Plant Sci.* 6, 86. doi: 10.3389/fpls.2015.00086

Wichard, T., Charrier, B., Mineur, F., Bothwell, J. H., De Clerck, O., and Coates, J. C. (2015). The green seaweed *Ulva*: a model system to study morphogenesis. *Front. Plant Sci.* 6, 72. doi: 10.3389/fpls.2015.00072

Wolf, M. A., Sciuto, K., Andreoli, C., and Moro, I. (2012). *Ulva* (Chlorophyta, ulvales) biodiversity in the north adriatic sea (Mediterranean, Italy): cryptic species and new introductions. *J. Phycol.* 48, 1510–1521. doi: 10.1111/jpy.12005

Woodhouse, K. O. W., and Zuccarello, G. C. (2023). Diversity of tropical macroalgae in the New Zealand marine aquarium trade. *New Z. J. Mar. Freshw. Res.* 57, 207–228. doi: 10.1080/00288330.2021.1975778

Woolcott, G. W., Iima, M., and King, R. J. (2000). Speciation within *Blidingia minima* (Chlorophyta) in Japan: evidence from morphology, ontogeny, and analyses of nuclear rDNA ITS sequence. *J. Phycol.* 36, 227–236. doi: 10.1046/j.1529-8817.2000.99034.x

Wu, M. X., Hu, Y., Wu, P. L., He, P. M., He, N., Zhang, B. L., et al. (2020). Does soil pore water salinity or elevation influence vegetation spatial patterns along coasts? A case study of restored coastal wetlands in Nanhui, Shanghai. *Wetlands* 40, 2691–2700. doi: 10.1007/s13157-020-01366-6

Wu, H. L., Liu, Y. M., Beardall, J., Zhong, Z. H., Gao, G., and Xu, J. T. (2022). Physiological acclimation of *Ulva prolifera* to seasonal environmental factors drives green tides in the Yellow Sea. *Mar. Environ. Res.* 179, 105695. doi: 10.1016/j.marenvres.2022.105695

Wu, M. X., Wu, P. L., He, P. M., He, N., Hu, Y., Wang, M. Q., et al. (2021). Theory of scale-dependent feedback: An experimental validation and its significance for coastal saltmarsh restoration. *Sci. Total. Environ.* 756, 143855. doi: 10.1016/j.scitotenv.2020.143855

Xia, Z. Y., Cao, X. L., Li, S., Cao, J. X., Tong, Y. C., Sun, Y. Q., et al. (2023c). Distribution of *Ulva prolifera*, the dominant species in green tides along the Jiangsu Province coast in the Southern Yellow Sea, China. *J. Sea. Res.* 196, 102436. doi: 10.1016/j.seares.2023.102436

Xia, P., Feng, A. P., and Zhao, M. W. (2022b). *Source zoning and quality status of surface sediments in typical intertidal zones of China* (Beijing: Science Press), 1–234.

Xia, Z. Y., Liu, J. L., Zhao, S., Cui, Q. W., Bi, F. L., Zhang, J. H., et al. (2023b). Attached *Ulva meridionalis* on nearshore dikes may pose a new ecological risk in the Yellow Sea. *Environ. pollut.* 332, 121969. doi: 10.1016/j.envpol.2023.121969

Xia, Z. Y., Liu, J. L., Zhao, S., Sun, Y. Q., Cui, Q. W., Wu, L. J., et al. (2024a). Review of the development of the green tide and the process of control in the southern Yellow Sea in 2022. *Estuar. Coast. Shelf. Sci.* 302, 108772. doi: 10.1016/j.ecss.2024.108772

Xia, Z. Y., Yang, Y. T., Zeng, Y. Q., Sun, Y. Q., Cui, Q. W., Chen, Z. H., et al. (2024b). Temporal succession of micropropagules during accumulation and dissipation of green tide algae: A case study in Rudong coast, Jiangsu Province. *Mar. Environ. Res.* 202, 106719. doi: 10.1016/j.marenvres.2024.106719

Xia, Z. Y., Yuan, H. Q., Liu, J. L., Sun, Y. Q., Tong, Y. C., Zhao, S., et al. (2022a). A review of physical, chemical, and biological green tide prevention methods in the Southern Yellow Sea. *Mar. pollut. Bull.* 180, 113772. doi: 10.1016/j.marpolbul.2022.113772

Xia, Z. Y., Yuan, H. Q., Liu, J. L., Zhao, S., Tong, Y. C., Sun, Y. Q., et al. (2023a). Biomass and species composition of green macroalgae in the Binhai Harbor intertidal zone of the Southern Yellow Sea. *Mar. pollut. Bull.* 186, 114407. doi: 10.1016/j.marpolbul.2022.114407

Xiao, J., Wang, Z. L., Liu, D. Y., Fu, M. Z., Yuan, C., and Yan, T. (2021). Harmful macroalgal blooms (HMBs) in China's coastal water: Green and golden tides. *Harmful. Algae.* 107, 102061. doi: 10.1016/j.hal.2021.102061

Xiao, J., Zhang, X. H., Gao, C. L., Jiang, M. J., Li, R. X., Wang, Z. L., et al. (2016). Effect of temperature, salinity and irradiance on growth and photosynthesis of *Ulva prolifera*. *Acta Oceanol. Sin.* 35, 114–121. doi: 10.1007/s13131-016-0891-0

Xing, Q. G., An, D. Y., Zheng, X. Y., Wei, Z. N., Wang, X. H., Li, L., et al. (2019). Monitoring seaweed aquaculture in the Yellow Sea with multiple sensors for managing the disaster of macroalgal blooms. *Remote Sens. Environ.* 231, 111279. doi: 10.1016/j.rse.2019.111279

Xing, Q. G., and Hu, C. M. (2016). Mapping macroalgal blooms in the Yellow Sea and East China Sea using HJ-1 and Landsat data: Application of a virtual baseline reflectance height technique. *Remote Sens. Environ.* 178, 113–126. doi: 10.1016/j.rse.2016.02.065

Xing, Q. G., Liu, H. L., Li, J. H., Hou, Y. Z., Meng, M. M., and Liu, C. L. (2023). A novel approach of monitoring *Ulva pertusa* green tide on the basis of UAV and deep learning. *Water* 15, 3080. doi: 10.3390/w15173080

Xu, D., Gao, Z. Q., Zhang, X. W., Fan, X., Wang, Y. T., Li, D. M., et al. (2012). Allelopathic interactions between the opportunistic species *Ulva prolifera* and the native macroalga *Gracilaria lichvoides*. *PloS One* 7, e33648. doi: 10.1371/journal.pone.0033648

Xu, Z. H., Meng, W. C., Li, S. Q., and Shan, J. Z. (2023). Residents' preference for the management of green tides and its determinants: The evidence from Qingdao, China. *Ocean. Coast. Manage.* 233, 106445. doi: 10.1016/j.ocecoaman.2022.106445

Xu, Z. H., Xu, J., Li, S. Q., and Wang, C. W. (2024). The influencing factors of residents' willingness to pay in marine ecological restoration: The integration of the theory of planned behavior and social capital theory. *Mar. Policy* 161, 106031. doi: 10.1016/j.marpol.2024.106031

Yan, H., Dai, Z. J., Li, J. F., Zhao, J. C., Zhang, X. L., and Zhao, J. K. (2011). Distributions of sediments of the tidal flats in response to dynamic actions, Yangtze (Changjiang) Estuary. *J. Geograph. Sci.* 21, 719–732. doi: 10.1007/s11442-011-0875-0

Yang, Y. (2017). *Reclamation Effects on Macrobenthos in Dongtan Wetland of Nanhui District in Shanghai* (Shanghai: East China Normal University), 1–73.

Yang, S. L., Milliman, J. D., Li, P., and Xu, K. (2011). 50,000 dams later: Erosion of the Yangtze River and its delta. *Global Planetary. Change* 75, 14–20. doi: 10.1016/j.gloplacha.2010.09.006

Yong, W. T. L., Thien, V. Y., Rupert, R., and Rodrigues, K. F. (2022). Seaweed: A potential climate change solution. *Renewable Sustain. Energy Rev.* 159, 112222. doi: 10.1016/j.rser.2022.112222

You, D., Tong, C. F., and Wu, F. R. (2018). Effects of sediment erosion and deposition variation on the benthic macroinvertebrate functional groups in an intertidal salt marsh of Nanhui Dongtan during the dry season, Changjiang River Estuary. *Haiyang. Xuebao.* 40, 63–78. doi: 10.3969/j.issn.0253-4193.2018.08.007

Yu, D. F., Li, J. M., Xing, Q. G., An, D. Y., and Li, J. H. (2023). The dynamics of floating macroalgae in the east China sea and its vicinity waters: A comparison between 2017 and 2023. *Water* 15, 3797. doi: 10.3390/w15213797

Zhang, B. (2012). *Influence of land use changes on waterbirds after coastal wetland reclamation in the Yangtze River Estuary: a case study of Nanhui Dongtan area* (Shanghai: East China Normal University), 1–51.

Zhang, W. X., Dunne, J. P., Wu, H., and Zhou, F. (2022). Regional projection of climate warming effects on coastal seas in east China. *Environ. Res. Lett.* 17, 074006. doi: 10.1088/1748-9326/ac7344

Zhang, S., Hu, C. M., Barnes, B. B., and Harrison, T. N. (2022). Monitoring *Sargassum* inundation on beaches and nearshore waters using planetScope/dove observations. *IEEE Geosci. Remote Sens. Lett.* 19, 1503605. doi: 10.1109/LGRS.2022.3148684

Zhang, J. H., Liu, C. C., Yang, L. L., Gao, S., Ji, X., Huo, Y. Z., et al. (2015). The source of the *Ulva* blooms in the East China Sea by the combination of morphological, molecular and numerical analysis. *Estuar. Coast. Shelf. Sci.* 164, 418–424. doi: 10.1016/j.ecss.2015.08.007

Zhang, Q. C., Yu, R. C., Chen, Z. F., Qiu, L. M., Wang, Y. F., Kong, F. Z., et al. (2018). Genetic evidence in tracking the origin of *Ulva prolifera* blooms in the Yellow Sea, China. *Harmful. Algae.* 78, 86–94. doi: 10.1016/j.hal.2018.08.002

Zhao, J., Jiang, P., Qiu, R., Ma, Y. Y., Wu, C. H., Fu, H. H., et al. (2018). The Yellow Sea green tide: A risk of macroalgae invasion. *Harmful. Algae.* 77, 11–17. doi: 10.1016/j.hal.2018.05.007

Zhao, Z. T., Li, M., Wu, T. J., Zhang, M. J., Shen, X. Y., Ma, S. Z., et al. (2024). Genetic diversity analysis of *Suaeda* plants in Shanghai coastal wetlands based on DNA barcode. *J. Shanghai. Ocean. Univ.*, 1–21. doi: 10.12024/jsou.20230704281

Zhao, Z. F., Liu, Z. Y., Qin, S., Wang, X. H., Song, W. L., Liu, K., et al. (2021). Impacts of low pH and low salinity induced by acid rain on the photosynthetic activity of green tidal alga *Ulva prolifera*. *Photosynthetica* 59, 468–477. doi: 10.32615/ps.2021.036

Zhao, S., Xia, Z. Y., Liu, J. L., Sun, J. Y., Zhang, J. H., and He, P. M. (2023). Morphology, growth, and photosynthesis of *Ulva prolifera* O.F. Müller (Chlorophyta, Ulvophyceae) gametophytes, the dominant green tide species in the Southern Yellow Sea. *J. Sea. Res.* 193, 102375. doi: 10.1016/j.seares.2023.102375